1975

A remotely controlled wind tunnel model for the demonstration of aircraft stability and control characteristics.

Merrill, John Christian

Monterey, California. Naval Postgraduate School

A REMOTELY CONTROLLED WIND TUNNEL MODEL FOR THE DEMONSTRATION OF AIRCRAFT STABILITY AND CONTROL CHARACTERISTICS

John Christian Merrill

NAVAL POSTGRADUATE SCHOOL
Monterey, California

THESIS

A REMOTELY CONTROLLED WIND TUNNEL MODEL
FOR THE DEMONSTRATION OF AIRCRAFT
STABILITY AND CONTROL CHARACTERISTICS

by

John Christian Merrill

June 1975

Thesis Advisor: H. L. Power

UNCLASSIFIED

SECURITY CLASSIFICATION OF THIS PAGE (When Data Entered)

REPORT DOCUMENTATION PAGE		READ INSTRUCTIONS BEFORE COMPLETING FORM
1. REPORT NUMBER	2. GOVT ACCESSION NO.	3. RECIPIENT'S CATALOG NUMBER
4. TITLE (and Subtitle) A Remotely Controlled Wind Tunnel Model for the Demonstration of Aircraft Stability and Control Characteristics		5. TYPE OF REPORT & PERIOD COVERED Master's Thesis; June 1975
		6. PERFORMING ORG. REPORT NUMBER
7. AUTHOR(s) John Christian Merrill		8. CONTRACT OR GRANT NUMBER(s)
9. PERFORMING ORGANIZATION NAME AND ADDRESS Naval Postgraduate School Monterey, California 93940		10. PROGRAM ELEMENT, PROJECT, TASK AREA & WORK UNIT NUMBERS
11. CONTROLLING OFFICE NAME AND ADDRESS Naval Postgraduate School Monterey, California 93940		12. REPORT DATE June 1975
		13. NUMBER OF PAGES
14. MONITORING AGENCY NAME & ADDRESS(if different from Controlling Office) Naval Postgraduate School Monterey, California 93940		15. SECURITY CLASS. (of this report) Unclassified
		15a. DECLASSIFICATION/DOWNGRADING SCHEDULE

16. DISTRIBUTION STATEMENT (of this Report)

Approved for public release; distribution unlimited.

17. DISTRIBUTION STATEMENT (of the abstract entered in Block 20, if different from Report)

18. SUPPLEMENTARY NOTES

19. KEY WORDS (Continue on reverse side if necessary and identify by block number)

Stability and Control

Wind Tunnel Model

20. ABSTRACT (Continue on reverse side if necessary and identify by block number)

A remotely controlled wind tunnel model with degrees of freedom in roll, pitch, and yaw was designed and constructed to demonstrate some of the major dynamic stability and control characteristics of a full scale aircraft. The longitudinal characteristics of the model were examined, and it was found that the response to a step function input deflection of the horizontal tail could be predicted accurately.

A Remotely Controlled Wind Tunnel Model for the Demonstration of Aircraft Stability and Control Characteristics

by

John Christian Merrill
Ensign, United States Navy
B.S.A.E., United States Naval Academy, 1974

Submitted in partial fulfillment of the
requirements for the degree of

MASTER OF SCIENCE IN AERONAUTICAL ENGINEERING

from the

NAVAL POSTGRADUATE SCHOOL
June 1975

ABSTRACT

A remotely controlled wind tunnel model with degrees of freedom in roll, pitch, and yaw was designed and constructed to demonstrate some of the major dynamic stability and control characteristics of a full scale aircraft. The longitudinal characteristics of the model were examined, and it was found that the response to a step function input deflection of the horizontal tail could be predicted accurately.

TABLE OF CONTENTS

LIST OF FIGURES

LIST OF SYMBOLS

a	Lift curve slope
a_t	Horizontal tail lift curve slope
b	Wing span
$\bar{c}$	Mean aerodynamic chord of the wing
C_{l_p}	Variation of rolling moment coefficient with roll rate perturbations
C_{l_r}	Variation of rolling moment coefficient with yaw rate perturbations
C_{l_β}	Variation of rolling moment coefficient with sideslip angle
$C_{l_{\delta_F}}$	Variation of rolling moment coefficient with vertical tail perturbation angle
C_{l_ξ}	Variation of rolling moment coefficient with aileron perturbation angle
C_{m_q}	Variation of pitching moment coefficient with pitch rate perturbations
C_{m_α}	Variation of pitching moment coefficient with angle of attack
$C_{m_{\dot\alpha}}$	Variation of pitching moment coefficient with time rate of change in angle of attack
$C_{m_{\alpha_t}}$	Variation of pitching moment coefficient with tail angle of attack perturbations
C_{n_p}	Variation of yawing moment coefficient with roll rate perturbations
C_{n_r}	Variation of yawing moment coefficient with yaw rate perturbations
C_{n_β}	Variation of yawing moment coefficient with sideslip angle
$C_{n_{\delta_F}}$	Variation of yawing moment coefficient with vertical tail perturbation angle

C_{n_ξ} Variation of yawing moment coefficient with aileron perturbation angle

D Denotes the derivative of a quantity with respect to nondimensional time

h C.G. position, fraction of the mean aerodynamic chord

h_n Neutral point of the model, fraction of the mean aerodynamic chord

i_A Nondimensional moment of inertia of the model about the X axis

i_B Nondimensional moment of inertia of the model about the Y axis

i_C Nondimensional moment of inertia of the model about the Z axis

i_E Nondimensional product of inertia of the model about the Y axis

l_t Distance from the C.G. to the horizontal tail aerodynamic center

l_v Distance from the C.G. to the vertical tail aerodynamic center

$\hat{p}$ Roll rate perturbation

$\hat{q}$ Pitch rate perturbation

$\hat{r}$ Yaw rate perturbation

S Wing area

S_t Horizontal tail area

S_v Vertical tail area

$\hat{U}$ Perturbations of airspeed in the X direction

V_H Horizontal tail volume ratio, $(l_t S_t)/(\bar{c}\ S)$

V_V Vertical tail volume ratio, $(l_v S_v)/(b\ S)$

Greek Symbols

α	Angle of attack
α_t	Perturbation of the horizontal tail angle
β	Sideslip angle
δ_F	Perturbation of the vertical tail angle
ζ	Damping ratio
η	Perturbation of the elevator angle
μ	Friction Coefficient
ξ	Perturbation of the aileron angle
ω_n	Undamped natural frequency

Superscripts

$\cdot$	Variation of the quantity with respect to time

ACKNOWLEDGEMENT

The author would like to express his thanks to Mr. Ronald Ramaker and Mr. Glenn Middleton of the Aerospace Department's wood and metal working shops for their time and effort in the actual construction of this model and its related components.

I. INTRODUCTION

In the opinion of the author, in order for a student to realize full benefit from any classroom learning process, that process should contain, whenever possible, some type of functional visual aid or laboratory to supplement and support the in-class lecture periods. The purpose of the design and construction of the stability and control wind tunnel model described in this thesis was to provide that additional support element to the stability and control courses offered at the Naval Postgraduate School, Monterey, California.

Although it was not possible to incorporate all of the degrees of freedom of an actual aircraft into the model, the model was designed to demonstrate many of the major dynamic characteristics of a full scale aircraft. The response of the model differs somewhat from that of an actual aircraft due to the fact that it must be supported within the wind tunnel test section and prohibited from translating in any of the three coordinate functions (Fig. I-1). This difference, however, is slight and does not detract from the primary purpose of the model.

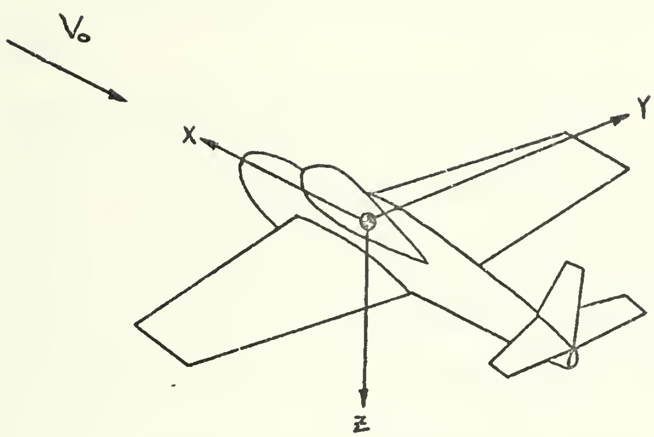

Figure I-1.

Model Reference Stability Axis System

II. MODEL DESCRIPTION

A. GENERAL FEATURES

The model (Fig. II-1) was designed to illustrate the characteristics of a typical single engine mid-wing aircraft. With minor modifications, however, the effects of various wing geometries can be studied because the model was designed with a removable wing section. Similarly, model tail sizes and shapes are variable. By the use of various wing and tail geometries the stability characteristics of the model may be changed.

Model attitude was controlled by the deflection of ailerons, and by horizontal and vertical tail deflections. The horizontal and vertical tails were designed as "all flying" surfaces so as to eliminate the need for separate elevator and rudder sections. The control surfaces are controlled from outside the tunnel by means of a remote control transmitter. A receiver mounted within the model receives the signals from the transmitter and, by means of mechanical linkage, a servo deflects the appropriate surface for control (Fig. II-2).

The resulting model motion was detected by three potentiometers which were situated so as to determine the angular rotation of the model about the X, Y, and Z stability axes. The potentiometer output was connected to a chart recorder which supplied a graphical history

of the model response. The motion sensor circuitry is shown in Figure II-3.

B. PHYSICAL MODEL DESCRIPTION

1. Fuselage

The fuselage has an overall length of 29 inches and was of circular cross section. It has a maximum outside diameter of 4-1/2 inches and a fineness rate of 6.44. The fuselage is constructed from a block of mahogany which was hollowed to give a wall thickness of 1/4 inch.

2. Wing

The wing is constructed of mahogany and has an NACA 2415 airfoil section, 6 degrees of dihedral, and no geometric twist. The wing has a span of 30 inches, a leading edge sweep of 23.5 degrees, and a taper ratio of .3. The left and right wing panels are attached to the fuselage by means of a carry through section (Fig. II-4) which also houses the main support bearing (Fig. II-5). The rectangular holes in the carry through section were cut to reduce the weight of the unit.

Ailerons, which are 8 inches long and 1 inch wide, were cut from the trailing edge of each of the wing panels. The total aileron area is 13.33 per cent of the wing area.

3. Horizontal and Vertical Tails

Both horizontal and vertical tail surfaces are constructed of mahogany and have an NACA 0012 airfoil section. The tails are designed as slab surfaces so as to

eliminate the necessity for separate elevator and rudder sections. The tail surfaces are held stationary on rotating axles by means of set screws. The axles are in turn supported by the ball bearing tail unit assembly shown in Figure II-6.

The horizontal tail has an overall span of 12.8 inches with a leading edge sweep of 25.2 degrees and a taper ratio of .24. The horizontal tail area is 26 per cent of the wing area.

The vertical tail height (from the fuselage centerline) is 6-1/2 inches, the leading edge sweep is 50 degrees, and the taper ratio is .31. A vertical tail area to wing area ratio of .22 is used.

C. MAIN SUPPORT BEARING

The model is supported by the gimbaled arrangement shown in Figure II-5. This unit is installed so that the pivot point of the bearing is located exactly 14-1/2 inches aft of the nose. This point serves as the origin for the model reference axes as well as the model center of gravity. Potentiometers incorporated within this unit detect model development in roll and pitch up to angles of 25 degrees. These potentiometers are used as voltage dividers, and their output voltage is connected to a chart recorder which provides a graphical measurement of the model response.

D. TAIL UNIT ASSEMBLY

The assembly shown in Figure II-6 serves to support the horizontal and vertical tail shafts which rotate the surfaces to the desired deflection angle. The unit is constructed of aluminum and contains four ball bearings (2 horizontal and 2 vertical) on which the tail axles are supported. The entire assembly is attached to the fuselage at a point such that the horizontal axle is exactly 12 inches aft of the model center of gravity. This resulted in a horizontal tail volume ratio, V_H, of .732, and a vertical tail volume ratio, V_V, of .08.

E. WIND TUNNEL MOUNT

The model was supported in the wind tunnel test section by means of the mounting assembly shown in Figure II-7. This support was constructed of aluminum and was attached to the roof of the wind tunnel as shown in Figure II-8. It has an overall length of 12 inches of which approximately six inches protruded down into the tunnel flow. This portion of the support was shrouded by a symmetrical aerodynamic fairing.

The model was connected to the mounting unit through a 7/16 inch diameter stainless steel tube. The shaft of the main support bearing was inserted into the bottom of the tube and tightened in place with two set screws. Collars, in conjunction with thrust bearings located within the main unit, absorbed any lift, drag, and side forces of the

model while still allowing it to rotate freely about all the coordinate axes.

The shaft of a potentiometer located on top of the mounting unit was inserted into the top of the stainless steel tube and was held tight with a set screw. This potentiometer sensed yaw angle of the model, and a yaw stopper attached to the steel tube limited yaw to 30 degrees.

F. SUMMARY OF MODEL DIMENSIONS

Wing:

Area (including portion covered by fuselage)	120 in^2
Span	30 in
Chord-root	6.15 in.
-tip	1.85 in
-MAC	4.38 in
Aspect Ratio	7.5
Airfoil Section	NACA 2415
Leading Edge Sweep	23.5°
Dihedral Angle	6°

Horizontal Tail:

Area (including portion covered by fuselage)	31.1 in^2
Span	12.8 in
Chord-root	3.94 in
-tip	.93 in
Aspect Ratio	5.27
Airfoil Section	NACA 0012

Leading Edge Sweep	25.2°
Incidence (variable)	10°
Tail Volume Ratio	.732

Vertical Tail:

Area (including portion covered by fuselage)	26 in^2
Height (from fuselage centerline)	6.5 in
Chord-root	6.5 in
-tip	1.5 in
Airfoil Section	NACA 0012
Leading Edge Sweep	50°
Tail Volume Ratio	.08

Fuselage:

Total Length	29 in
Maximum Cross Sectional Area	16 in^2
Fineness Ratio	6.44

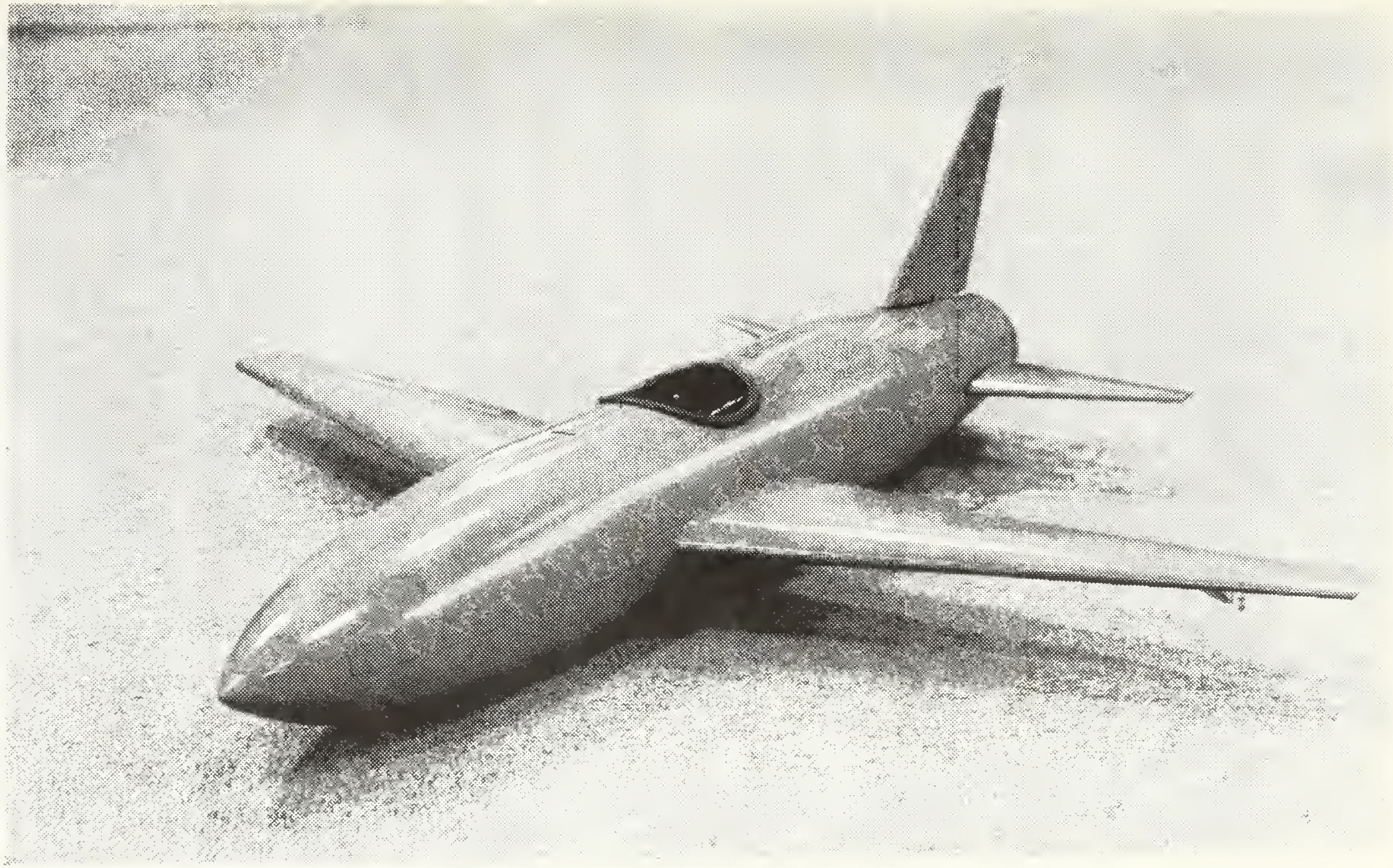

Figure II-1. Model Configuration

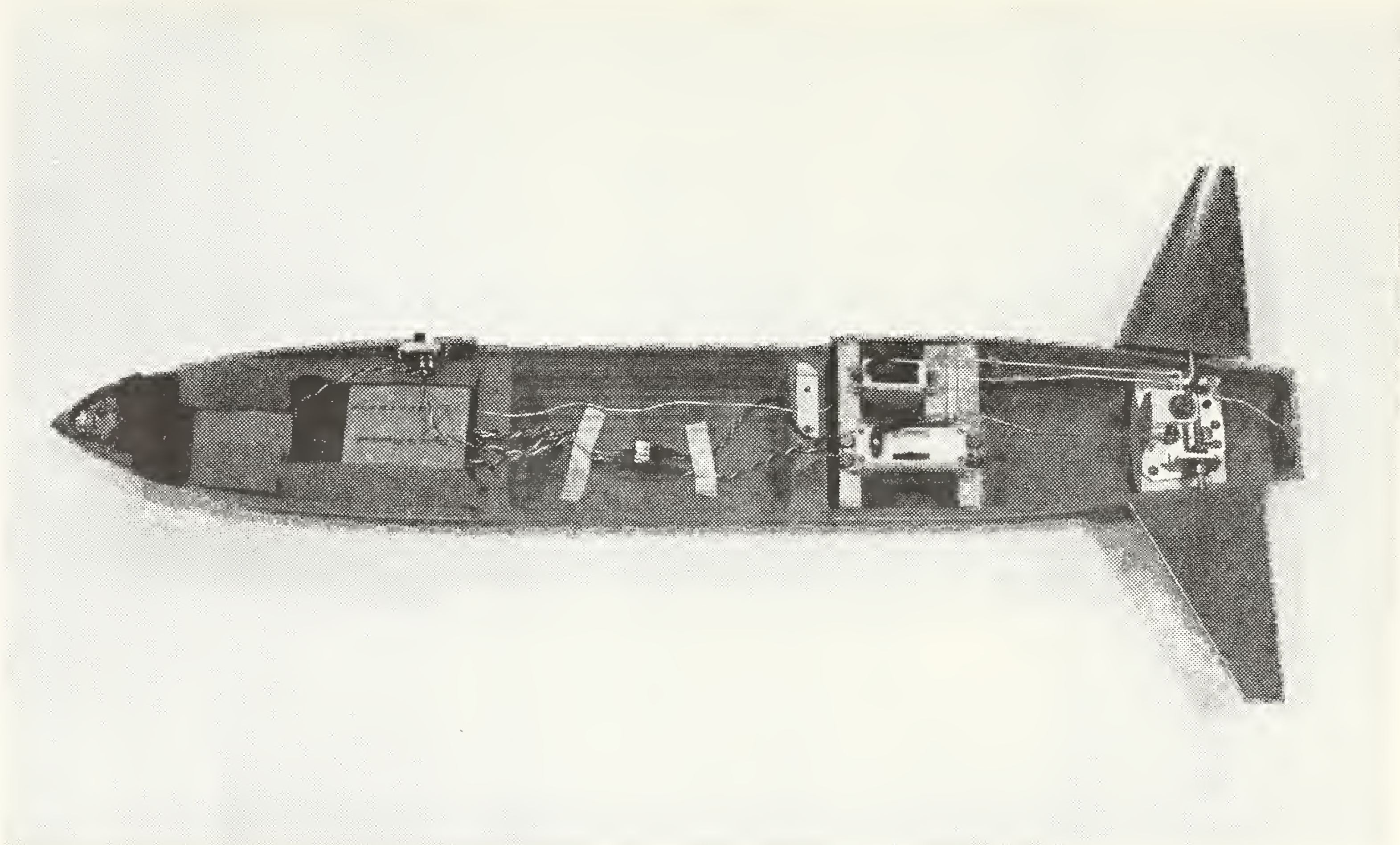

Figure II-2. Model Internal Components Showing the Receiver and Horizontal and Vertical Tail Servos

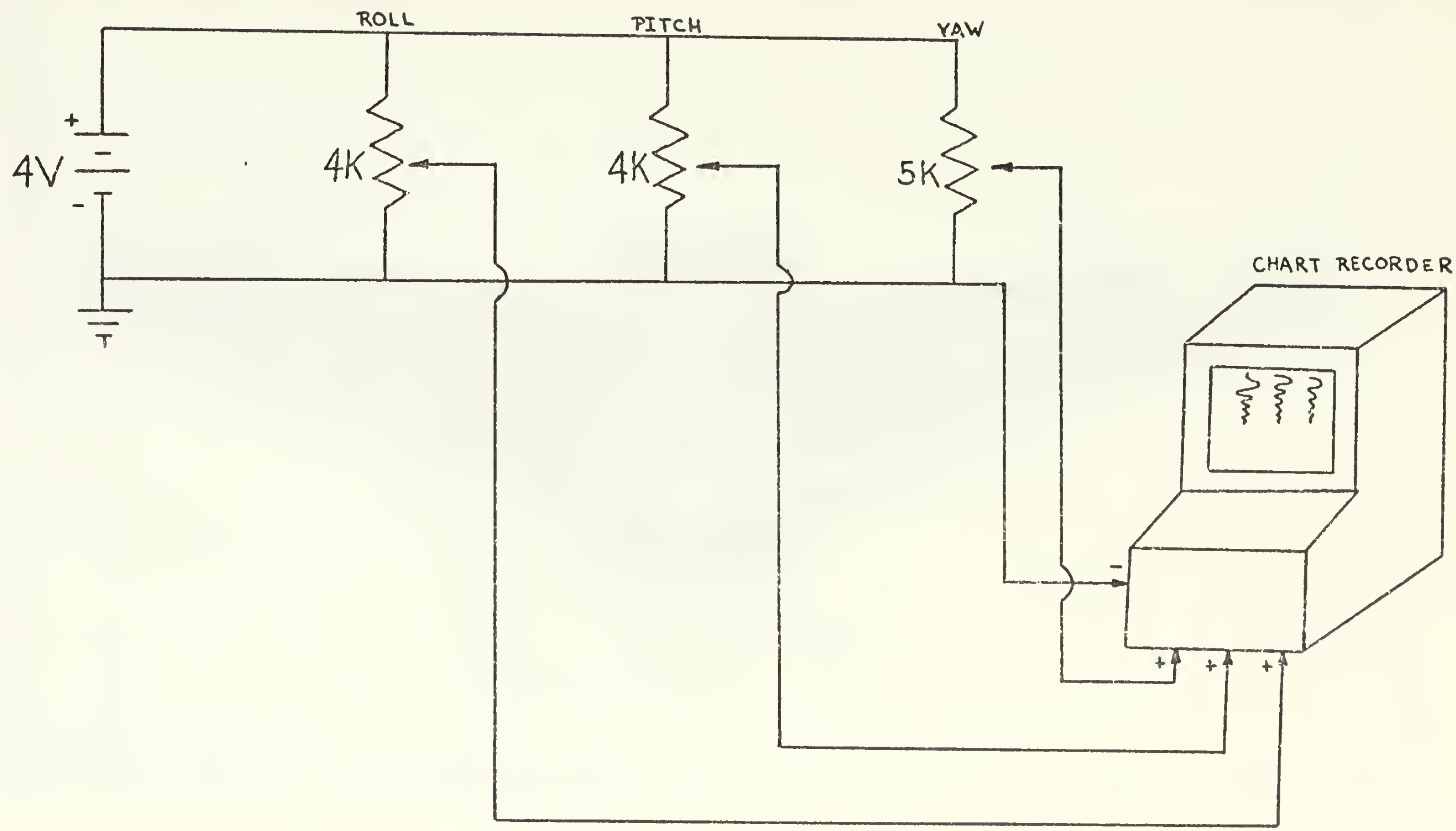

Figure II-3. Motion Sensor Circuitry

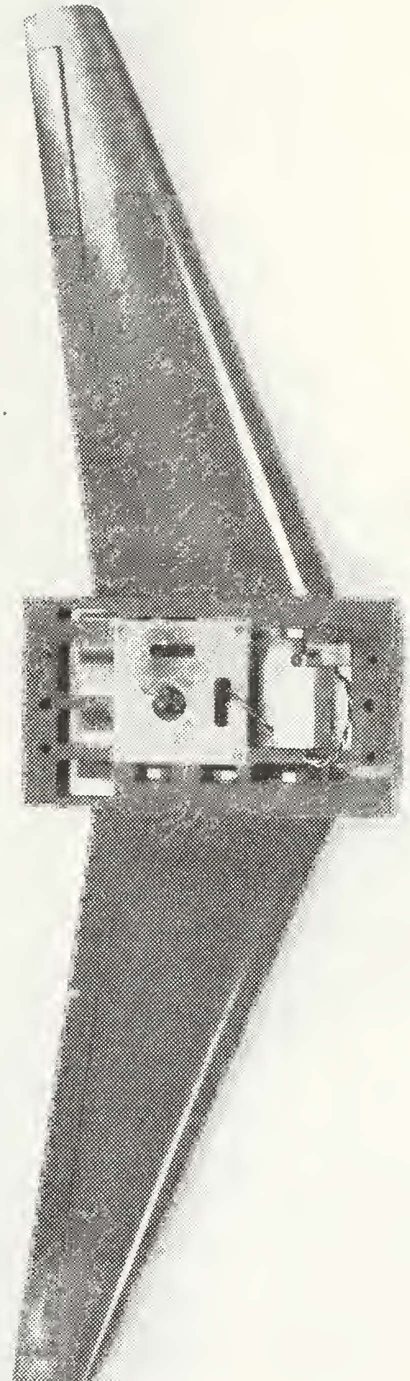

Figure II-4. Wing Section

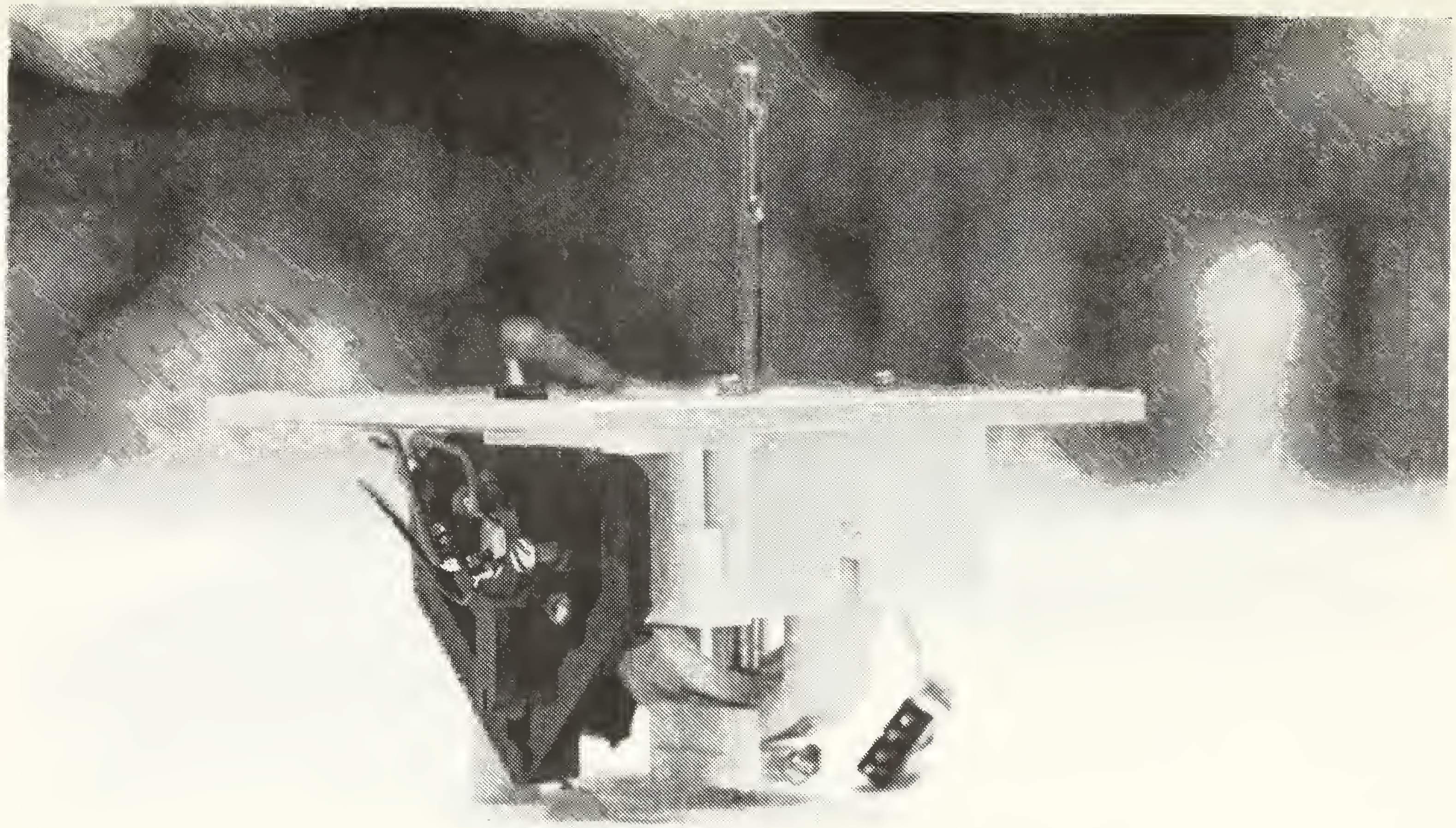

Figure II-5. Main Support Bearing

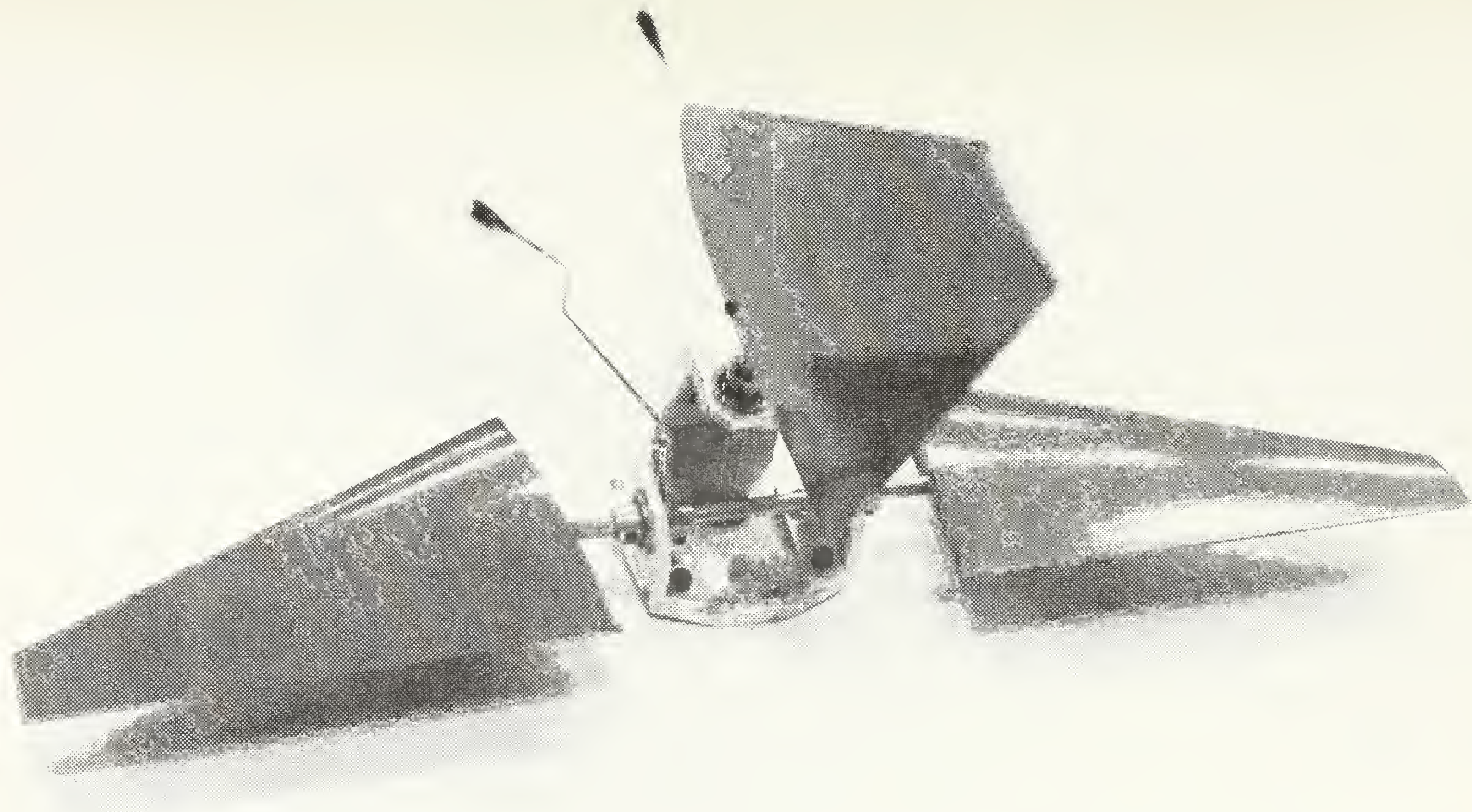

Figure II-6. Tail Unit Assembly with Tail Surfaces Installed

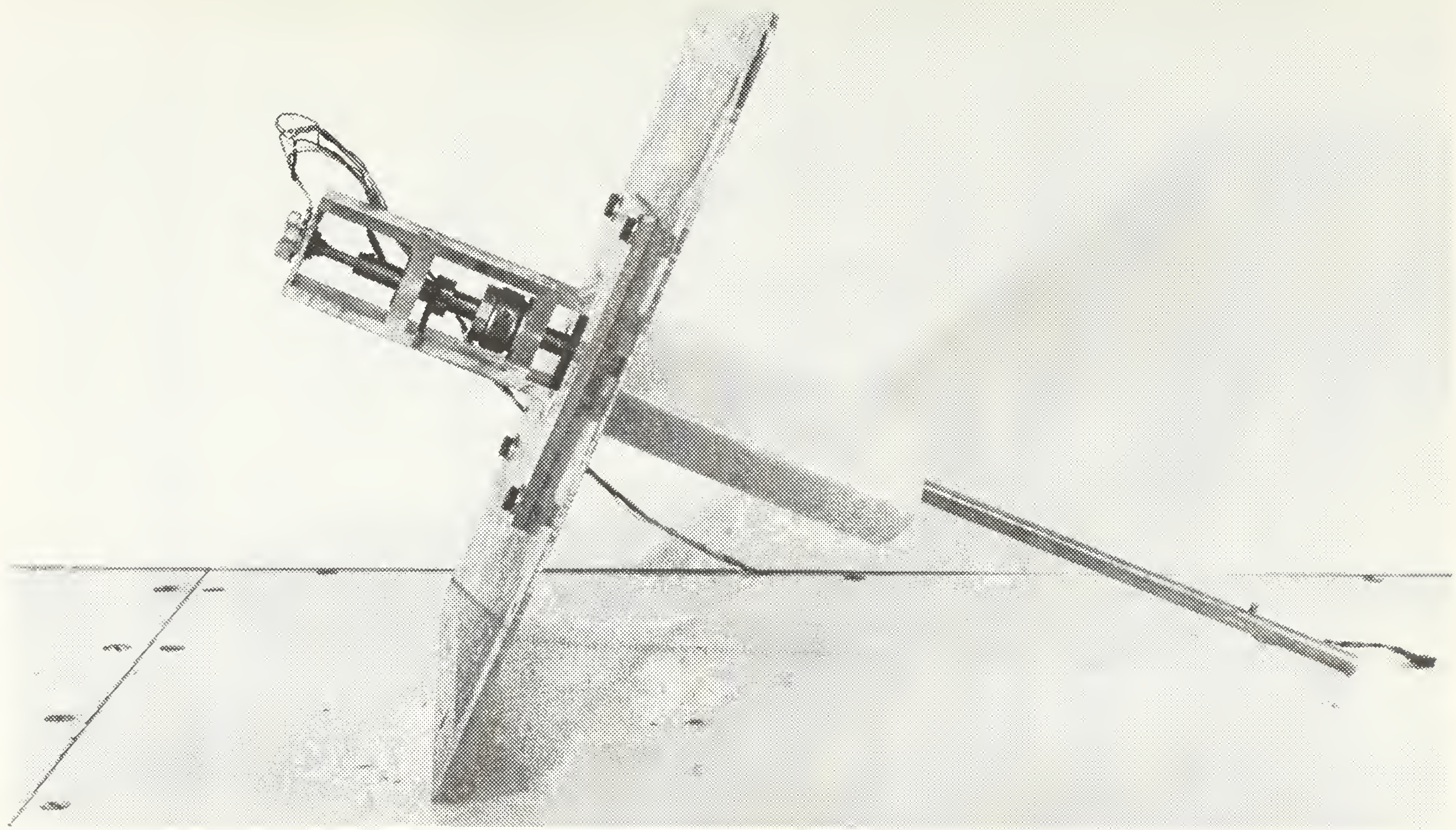

Figure II-7. Wind Tunnel Mount

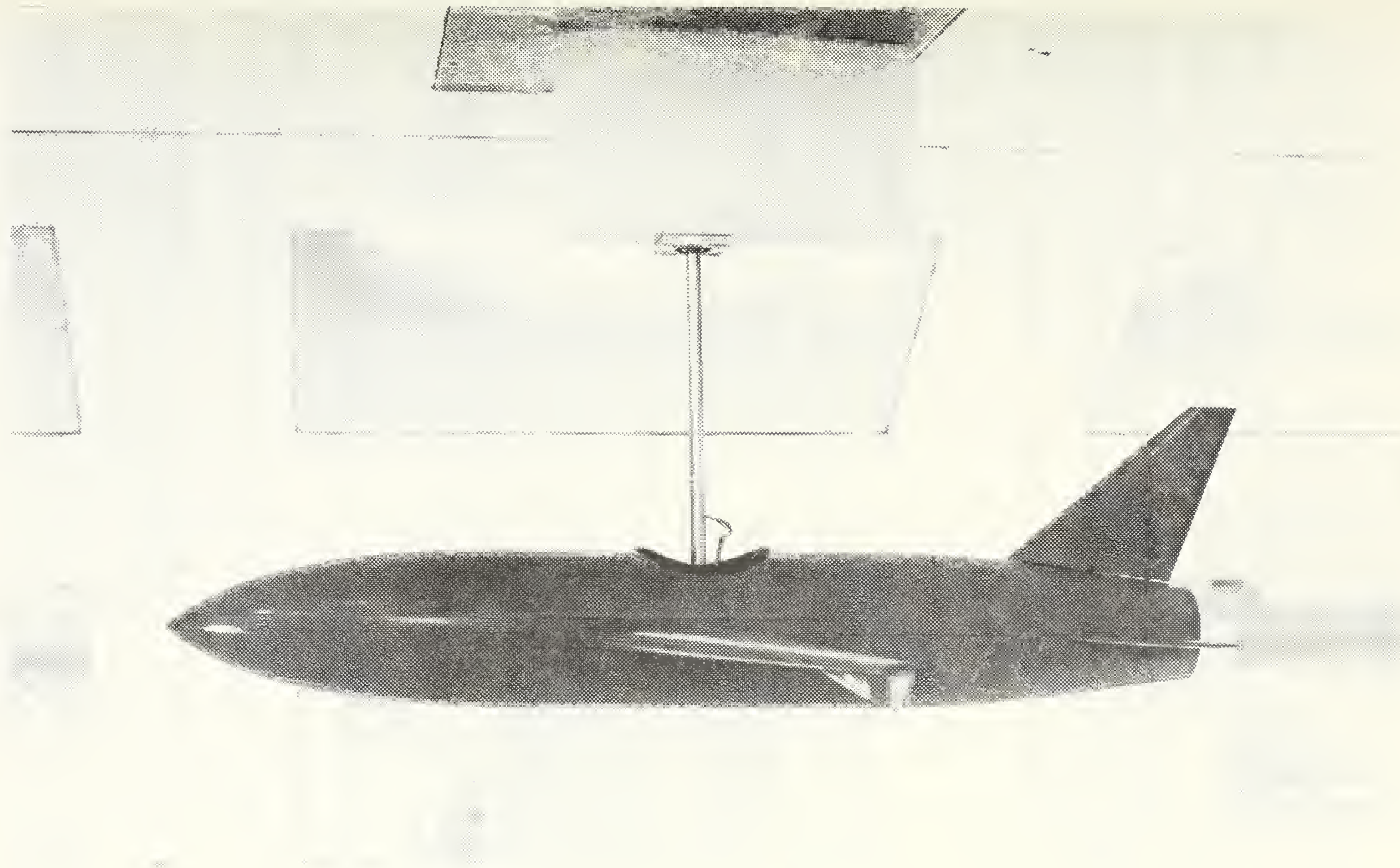

Figure II-8. Model Mounted in the Wind Tunnel

III. ANALYTICAL MODEL

The model was designed, and its motion predicted by means of linear equations of motion. From these equations it was possible to predict model response to various control surface inputs. Also, once these equations had been established, it was possible to theoretically vary model characteristics and obtain information on how this new configuration would respond.

A. LONGITUDINAL EQUATIONS OF MOTION

The nondimensional longitudinal equations of motion were obtained from Ref. 1. These equations were developed using the small disturbance theory for an aircraft having four degrees of longitudinal freedom. The model, however, was suspended in the wind tunnel so that translations along the X and Z axes were denied, thereby allowing the X and Z force equations to be neglected entirely. The elevator hinge moment equation was also neglected, as control displacement rather than control force was considered as an input.

Due to the assumptions of small angles and constant airstream velocity in the tunnel, perturbations of the velocity in the X direction, $\hat{U}$ terms, were zero. Also, the model was situated within the tunnel so that the flight path angle, θ, and the angle of attack, α, were equal.

Due to the fact that the horizontal tail was a slab surface and there was no separate elevator section, the quantity η which was originally defined as elevator perturbation angle was replaced by tail angle of attack α_t. It was further assumed that $\dot{\alpha}_t$ terms were negligible.

Applying the above assumptions to the initial equations of motion yielded the following longitudinal equations of motion for the model.

$$i_B\ddot{\alpha} - (C_{m_{\dot{\alpha}}} + C_{m_q})\,\dot{\alpha} - C_{m_\alpha}\,\alpha - C_{m_{\alpha_t}}\,\alpha_t = 0 \qquad \text{III-1}$$

$$q = \dot{\alpha} \qquad \text{III-2}$$

These equations, however, do not take into account the friction inherent in the main support bearing on which the model pivots. Therefore, they must be further modified to account for this frictional retarding moment.

The frictional moment present at the pivot is a function of model supporting force. More accurately:

$$M_{frict.} = \mu_1\,(W - L) \qquad \text{III-3}$$

where: μ_1 = coefficient of friction (in.)

W = model weight (lbs.)

L = model lift (lbs.)

Putting this equation in nondimensional format results in the following expression:

$$C_{m_f} = \frac{2\,\mu_1\,W}{\rho\,V^2 S\bar{c}} - \frac{\mu_1}{\bar{c}}\,C_{L_\alpha}\,\alpha \qquad \text{III-4}$$

where: ρ = air density (slugs/ft^3)

V = velocity (ft/sec)

The first term on the right hand side of equation III-4 is the constant break-out moment of the bearing for any given airspeed; therefore, the perturbation of the frictional moment coefficient during motion was given by:

$$\Delta C_{m_f} = \frac{-\mu_1}{\bar{c}}\,C_{L_\alpha}\,\alpha \qquad \text{III-5}$$

and the revised model longitudinal equations of motion are:

$$i_B\ddot{\alpha} - (C_{m_{\dot{\alpha}}} + C_{m_q})\,\dot{\alpha} - (C_{m_\alpha} - \frac{\mu_1}{\bar{c}}\,C_{L_\alpha})\,\alpha - C_{m_{\alpha_t}}\,\alpha_t = 0 \qquad \text{III-6}$$

$$q = \dot{\alpha} \qquad \text{III-7}$$

The basic rules for the formulation of state equations from ordinary differential equations [Ref. 2] were followed in order to obtain the state variable representation of the model longitudinal equations of motion:

$$\begin{bmatrix} \dot{q} \\ \dot{\alpha} \end{bmatrix} = \begin{bmatrix} (C_{m_q} + C_{m_{\dot{\alpha}}})/i_B & (C_{m_\alpha} - \frac{\mu_1}{\bar{c}} C_{L_\alpha})/i_B \\ 1 & 0 \end{bmatrix} \begin{bmatrix} q \\ \alpha \end{bmatrix}$$

$$+ \begin{bmatrix} (C_{m_{\alpha_t}})/i_B \\ 0 \end{bmatrix} \begin{bmatrix} \alpha_t \end{bmatrix} \qquad \text{III-8}$$

B. LATERAL EQUATIONS OF MOTION

As with the longitudinal case, the lateral nondimensional equations of motion were obtained from Ref. 1 and then modified to fit the explicit conditions of the model suspended within the wind tunnel. To begin with, the Y force equation was disregarded due to the fact that the model was restricted from translating along that axis. Also, the rudder and aileron hinge moment equations were neglected since control displacement rather than control force constituted the input. The term ζ in the original set of equations denoted rudder angle perturbation; however, this was replaced by δ_F since the vertical fin was designed and constructed as a slab surface. It was further assumed that all $\dot{\xi}$ and $\dot{\delta}_F$ terms were zero.

The model was suspended within the tunnel so that the rate of change of the bank angle, $\dot{\phi}$, and roll rate, $\hat{p}$, were

equal. Also, the rate of change of the sideslip angle, $\dot{\beta}$, was the negative of the yaw rate, $\hat{r}$.

Applying the above conditions to the initial equations of motion resulted in the following model lateral equations of motion.

$$-C_{l_\beta}\beta + (i_A D - C_{l_p})\hat{p} - (i_E D + C_{l_r})\hat{r} - C_{l_\xi}\xi - C_{l_{\delta_F}}\delta_F = 0 \qquad \text{III-9}$$

$$-C_{n_\beta}\beta - (i_E D + C_{n_p})\hat{p} + (i_C D - C_{n_r})\hat{r} - C_{n_\xi}\xi - C_{n_{\delta_F}}\delta_F = 0 \qquad \text{III-10}$$

$$\dot{\phi} = \hat{p} \qquad \text{III-11}$$

$$\dot{\beta} = -\hat{r} \qquad \text{III-12}$$

However, as before, these equations do not reflect the frictional moments present and must be modified to do so. Model side force is the major parameter contributing to the retarding frictional moments during model lateral motion. Therefore:

$$L_{frict.} = \mu_1 Y \qquad \text{III-13}$$

and

$$N_{frict.} = \mu_2 Y \qquad \text{III-14}$$

where: $L_{frict.}$ = frictional component of rolling moment (in-lbs.)

$N_{frict.}$ = frictional component of yawing moment (in-lbs.)

$\mu_{1,2}$ = coefficients of friction (in.)

Y = side force (lbs.)

The frictional coefficients μ_1 and μ_2 should be equal, but the coefficient for the yaw axis has a different value due to the contribution of the yaw potentiometer.

Putting these equations in nondimensional format results in the following expressions for the respective frictional moment perturbations.

$$\Delta C_{l_f} = \frac{\mu_1}{b} C_{y_\beta} \beta \qquad \text{III-15}$$

and

$$\Delta C_{n_f} = \frac{\mu_2}{b} C_{y_\beta} \beta \qquad \text{III-16}$$

where: b = wing span

Incorporating these contributions to the rolling and yawing moments into the previous set of equations results in the following corrected set of model lateral equations of motion.

$$- (C_{l_\beta} + \frac{\mu_1}{b} C_{y_\beta})\beta + (i_A D - C_{l_p})\hat{p} - (i_E D + C_{l_r})\hat{r}$$

$$-C_{l_\xi} \xi - C_{n_{\delta_F}} \delta_F = 0 \qquad \text{III-17}$$

$$- (C_{n_\beta} + \frac{\mu_2}{b} C_{y_\beta})\beta - (i_E D + C_{n_p})\hat{p} + (i_C D - C_{n_r})\hat{r}$$

$$- C_{n_\xi}\xi - C_{n_{\delta_F}}\delta_F = 0 \qquad \text{III-18}$$

$$\dot{\phi} = \hat{p} \qquad \text{III-19}$$

$$\dot{\beta} = -\hat{r} \qquad \text{III-20}$$

Putting these equations in standard state variable format produced the following matrix system.

$$\begin{bmatrix} \dot{p} \\ \dot{r} \\ \dot{\beta} \\ \dot{\phi} \end{bmatrix} = \begin{bmatrix} (i_C C_{1_p} + i_E C_{n_p})/J & (i_C C_{1_r} + i_E C_{n_r})/J & (i_C K + i_E H)/J & 0 \\ (i_A C_{n_p} + i_E C_{1_p})/J & (i_A C_{n_r} + i_E C_{1_r})/J & (i_A H + i_E K)/J & 0 \\ 0 & -1 & 0 & 0 \\ 1 & 0 & 0 & 0 \end{bmatrix} \begin{bmatrix} p \\ r \\ \beta \\ \phi \end{bmatrix}$$

$$+ \begin{bmatrix} (i_C C_{1_\xi} + i_E C_{n_\xi})/J & (i_C C_{1_{\delta_F}} + i_E C_{n_{\delta_F}})/J \\ (i_A C_{n_\xi} + i_E C_{1_\xi})/J & (i_A C_{n_{\delta_F}} + i_E C_{1_{\delta_F}})/J \\ 0 & 0 \\ 0 & 0 \end{bmatrix} \begin{bmatrix} \xi \\ \delta_F \end{bmatrix} \qquad \text{III-21}$$

where: $J = i_A i_C - i_E^2$

$K = (C_{1_\beta} + \frac{\mu_1}{b} C_{y_\beta})$

$h = (C_{n_\beta} + \frac{\mu_2}{b} C_{y_\beta})$

IV. STABILITY DERIVATIVE RELATIONSHIPS

In order for the equations of motion to be of any use in the design of the model, the individual stability derivatives were programmed and expressed in terms of the model physical characteristics. The following sections present the relationships used to compute the required stability derivatives.

A. LONGITUDINAL STABILITY DERIVATIVES

The values of the stability derivatives involved in the longitudinal system of equations were determined using the relationships presented in Ref. 1. These are:

$$C_{m_\alpha} = -a(h_n - h) \qquad \text{IV-1}$$

$$C_{m_q} = -2a_t\left(\frac{l_t}{\bar{c}}\right)V_H \qquad \text{IV-2}$$

$$C_{m_{\dot{\alpha}}} = C_{m_q}\frac{d\varepsilon}{d\alpha} \qquad \text{IV-3}$$

$$C_{m_{\alpha_t}} = -a_t\, V_H \qquad \text{IV-4}$$

where V_H is the horizontal tail volume ratio given by:

$$V_H = \frac{l_t S_t}{\bar{c}\ S}$$

From the above equations it is evident that the longitudinal characteristics of the model are very dependent upon the tail length (l_t) and the tail size (S_t), and that by varying the tail area, the longitudinal stability characteristics of the model may vary significantly. For the model under study in this paper:

$C_{m_\alpha} = -1.144$ $\qquad$ $C_{m_q} = -14.979$

$C_{m_{\dot\alpha}} = -6.231$ $\qquad$ $C_{m_{\alpha_t}} = -2.9448$

B. LATERAL STABILITY DERIVATIVES

Unlike the longitudinal case, the expressions for the lateral stability derivatives are very complex and unwieldy to use and program. The equations of Ref. 3 were used to estimate these derivatives and are given in Appendix A. For this particular model, the computer program solution had the following values:

$C_{l_\beta} = -.1254$ $\qquad$ $C_{n_\beta} = .07379$

$C_{l_p} = -.4381$ $\qquad$ $C_{n_p} = -.00251$

$C_{l_r} = .0437$ $\qquad$ $C_{n_r} = -.15384$

$C_{l_\xi} = .69934$ $\quad$ $C_{n_\xi} = -.001197$

$C_{l_{\delta_F}} = .05554$ $\quad$ $C_{n_{\delta_F}} = -.23747$

V. EXPERIMENTAL LONGITUDINAL RESPONSE

A. EQUIPMENT CALIBRATION

With a 4-volt potential across the sensor system, the pitch and roll potentiometers were calibrated using a clinometer, and the yaw potentiometer was calibrated using a protractor with the yaw stopper as a pointer. The resulting calibration curves are presented in this section as Figure V-1. The relationships between control surface deflections and transmitter stick angle were also measured and are presented in Figure V-2.

B. TEST PROCEDURE

The sensor system was energized, after which the wind tunnel was activated and set at the desired airspeed. The model was then trimmed out at a slight nose-up attitude. The horizontal tail surface was deflected and the model response to a step function input was observed and recorded.

Test runs at airspeeds of 50.7, 58.7, 65.4, and 71.7 ft/sec and tail angle changes of 3, 4, 5, and 6 degrees (positive tail angle is with the leading edge up) were accomplished. The graphical results of the model response to a tail deflection of 6 degrees are presented as typical in Figures V-3 through V-6.

From these results, it was possible to determine the values of the damping ratio, ζ, and the undamped natural frequency, ω_n, for the model at the different airspeeds.

Figures V-7 and V-8 clearly illustrate that as the tunnel speed is increased, the value of ω_n remains fairly constant, while the value of ζ decreases. This results in a gradual decline of the damping factor $2\zeta\omega_n$ as the airspeed is increased. This decline in the damping term is a consequence of the increased wing lift at the higher airspeeds which reduces the pivot force resulting in less bearing friction.

Equation III-6 was used to obtain the characteristic equation for the model and the following expression for ω_n and ζ were obtained as functions of the friction coefficient, μ_1.

$$\omega_n = \sqrt{\frac{-\left(C_{m_\alpha} - \frac{\mu_1}{\bar{c}} C_{L_\alpha}\right)}{i_B}} \qquad \text{V-1}$$

$$\zeta = \frac{-\left(C_{m_{\dot{\alpha}}} + C_{m_q}\right)}{2 i_B} \sqrt{\frac{i_B}{-C_{m_\alpha} + \frac{\mu_1}{\bar{c}} C_{L_\alpha}}} \qquad \text{V-2}$$

Figures V-9 and V-10 illustrate these relationships for this model assuming constant μ_1 values.

The experimental results were used to determine the unknown bearing friction coefficient, μ_1. It was found that a value of 1.75 was required to match the predicted and experimental values of ω_n. Figure V-8 shows the

resulting comparison values for the damping ratio. It is evident that as the tunnel speed increases the experimental and theoretical values show fair agreement.

From the various test runs completed it was found that tunnel speeds around 65 ft/sec exhibited the best characteristics for both visual observation and graphical data acquisition of model response. At velocities greater than 75 ft/sec considerable model buffeting occurs which tends to overshadow any data obtained. Conversely, at tunnel speeds under 50 ft/sec the model response is greatly inhibited by bearing friction, and the resulting heavily damped motion rarely has more than one oscillation.

C. CONCLUSIONS

The model studied has demonstrated that the basic concept of a remotely controlled stability and control wind tunnel test model is a valid one. It has been shown that for the longitudinal case, the damping and frequency of the model may be predicted quite accurately using linear equations of motion.

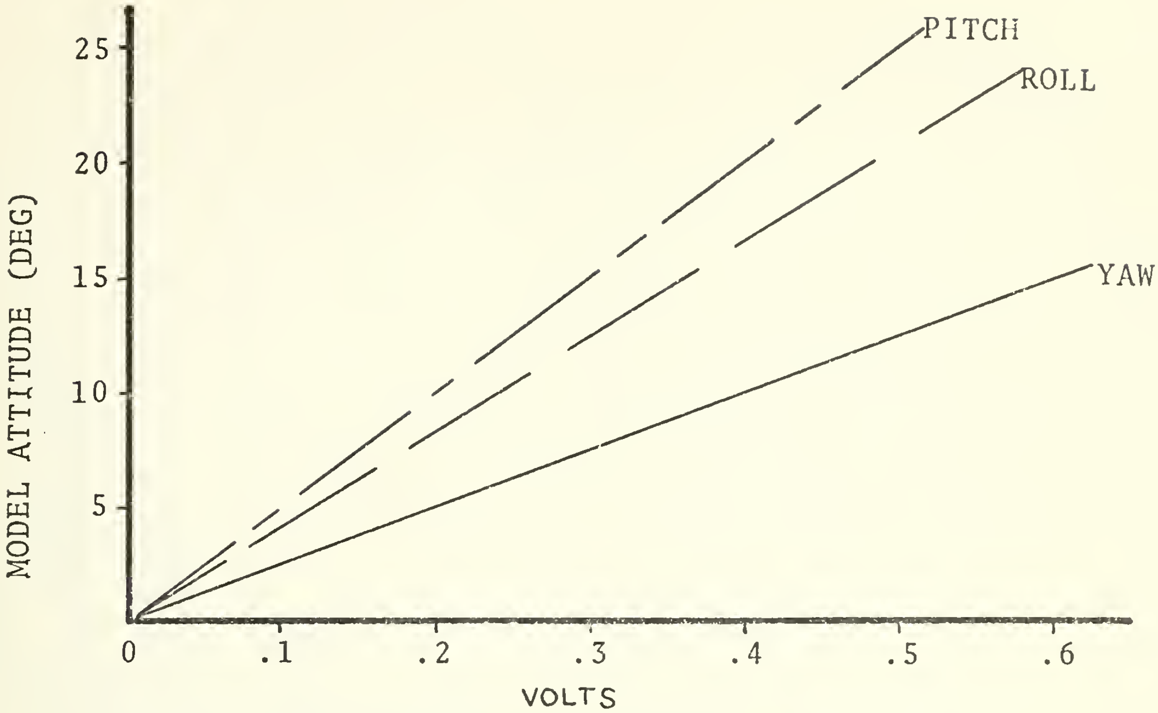

Figure V-1. Potentiometer Calibration Curves

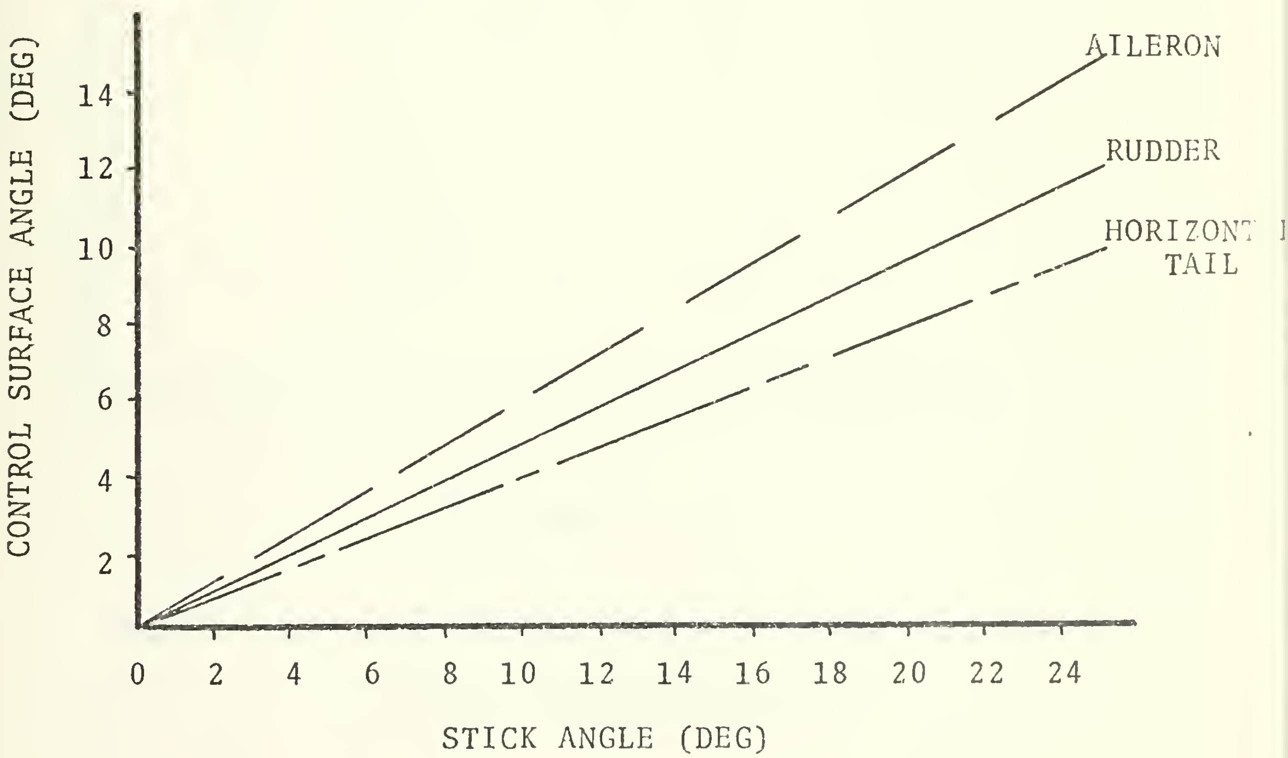

Figure V-2. Control Surface Angle vs. Transmitter Stick Angle

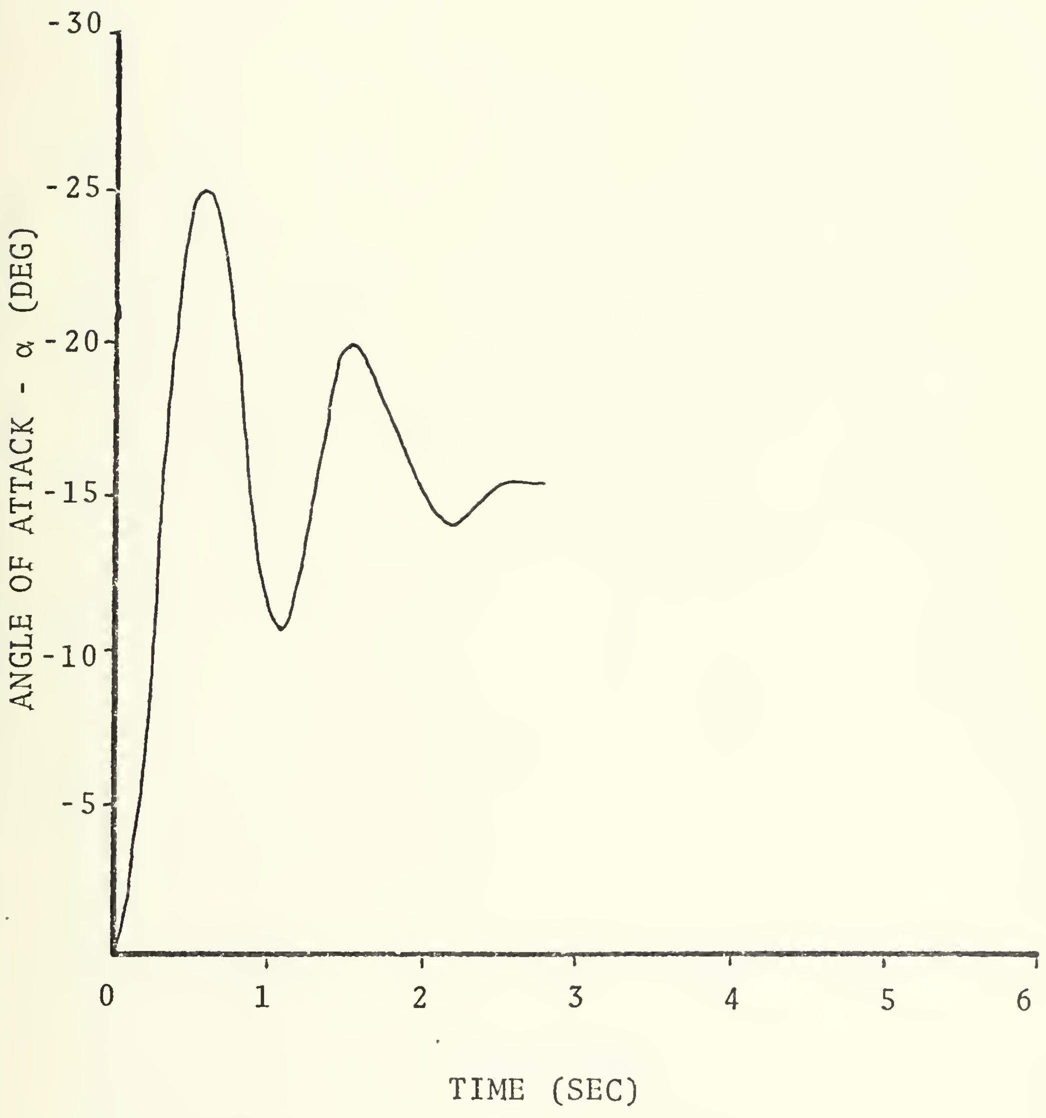

Figure V-3. Experimental Angle of Attack vs. Time

V_o = 50.7 ft/sec, $\Delta\alpha_t$ = 6°

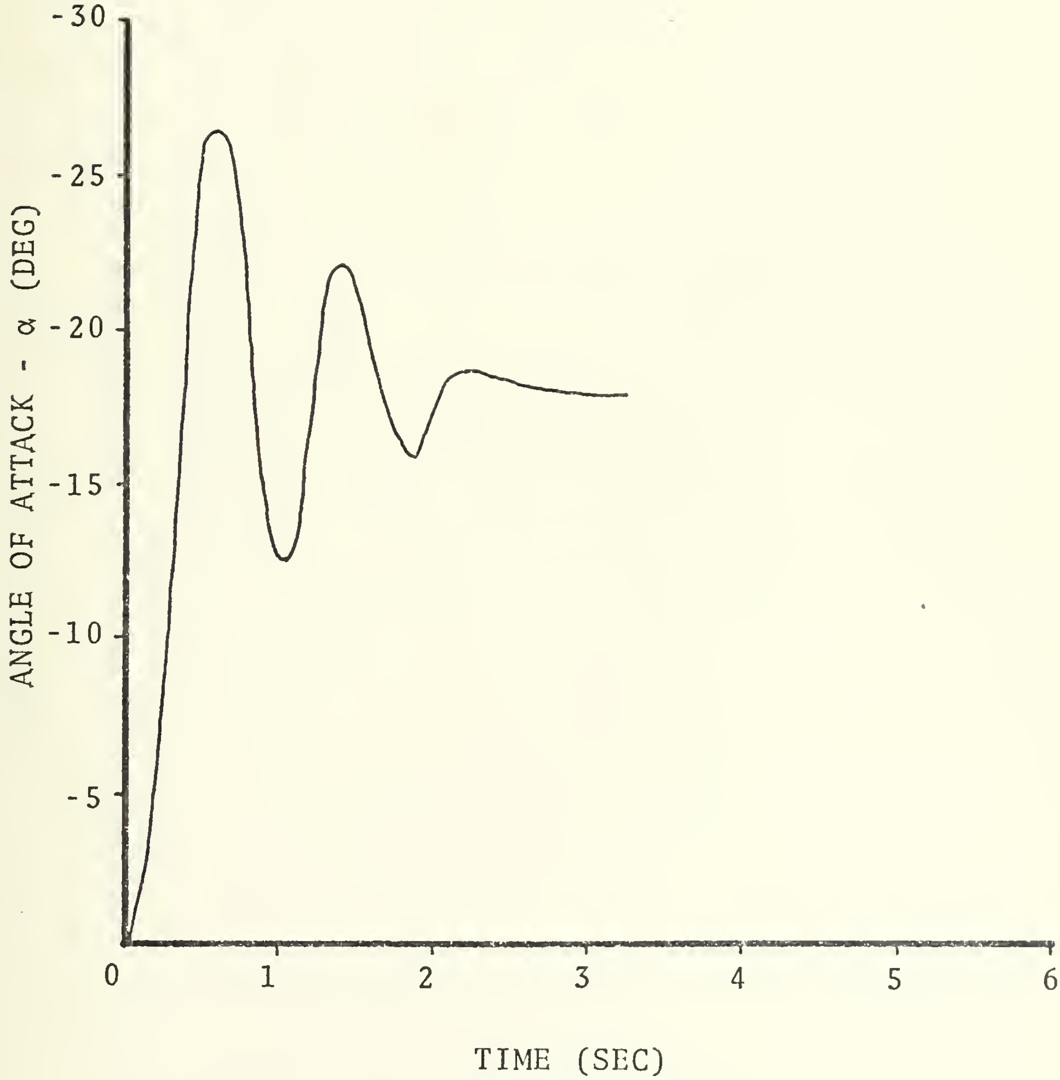

Figure V-4. Experimental Angle of Attack vs. Time

V_o = 58.7 ft/sec, $\Delta\alpha_t$ = 6°

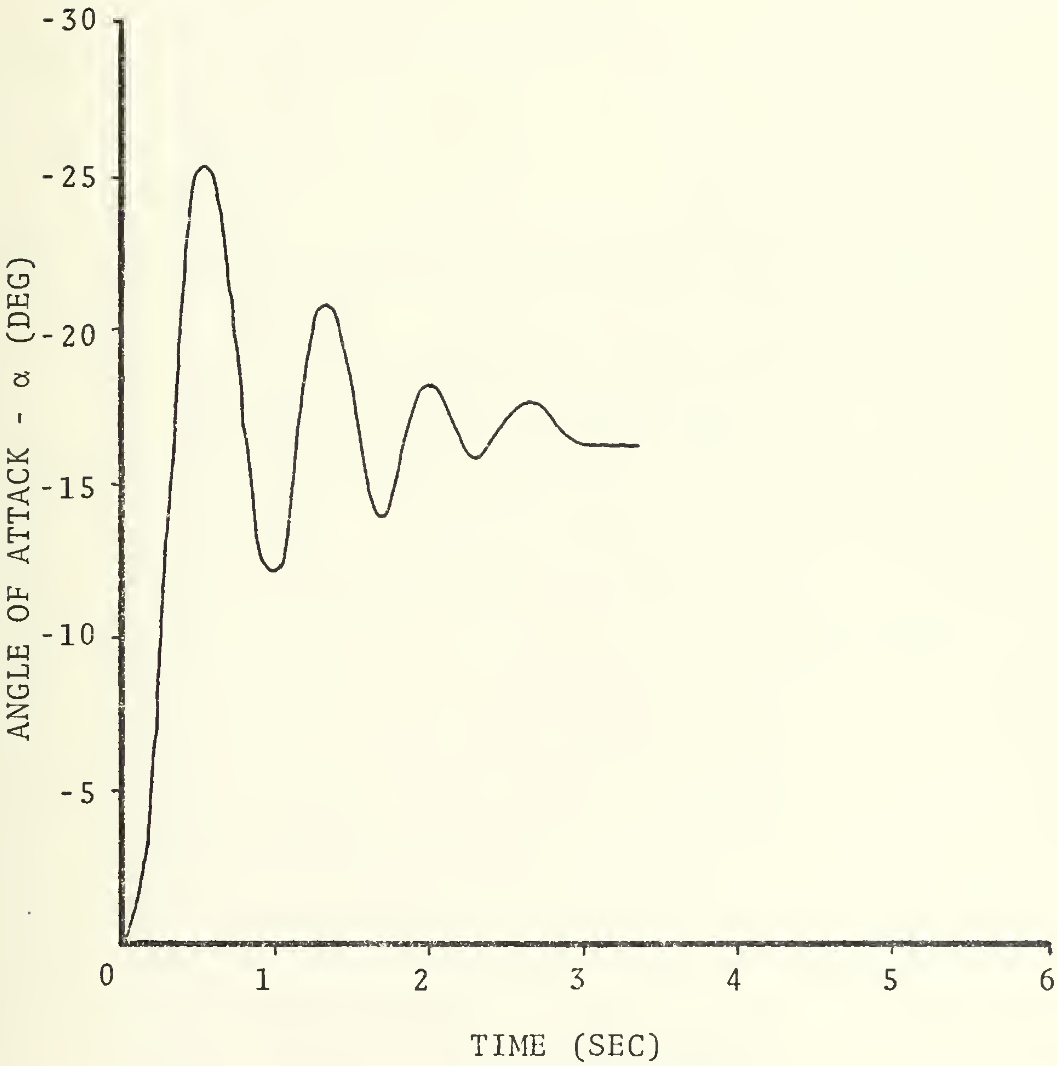

Figure V-5. Experimental Angle of Attack vs. Time

V_o = 65.4 ft/sec, $\Delta\alpha_t$ = 6°

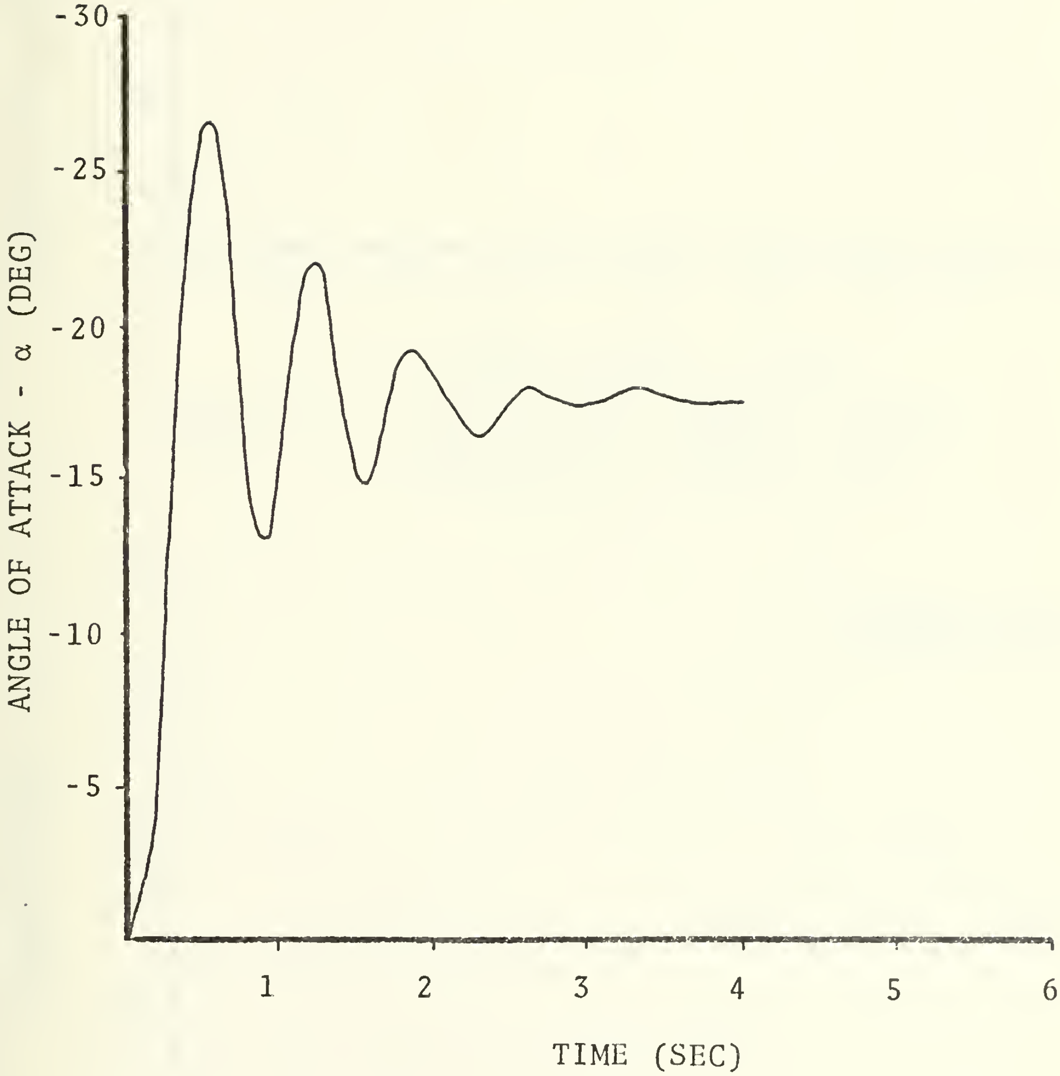

Figure V-6. Experimental Angle of Attack vs. Time

V_o = 71.7 ft/sec, $\Delta\alpha_t$ = 6°

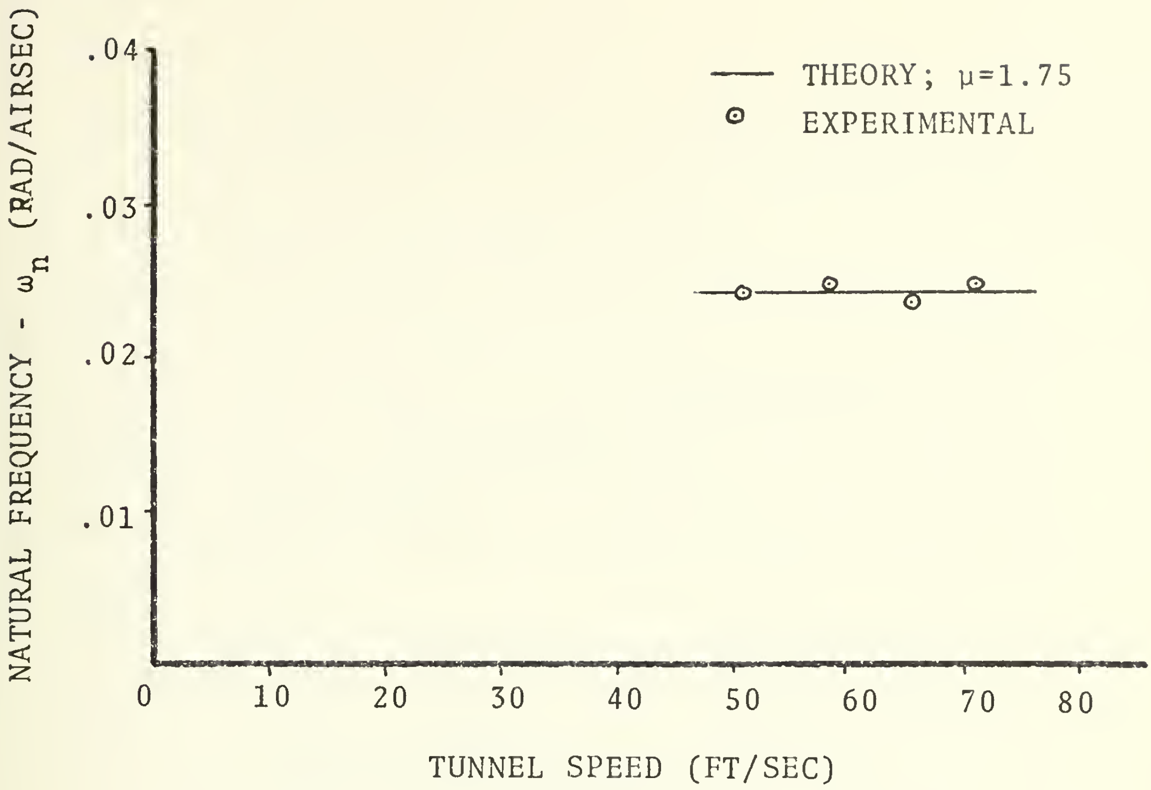

Figure V-7. Longitudinal Undamped Natural Frequency vs. Tunnel Speed

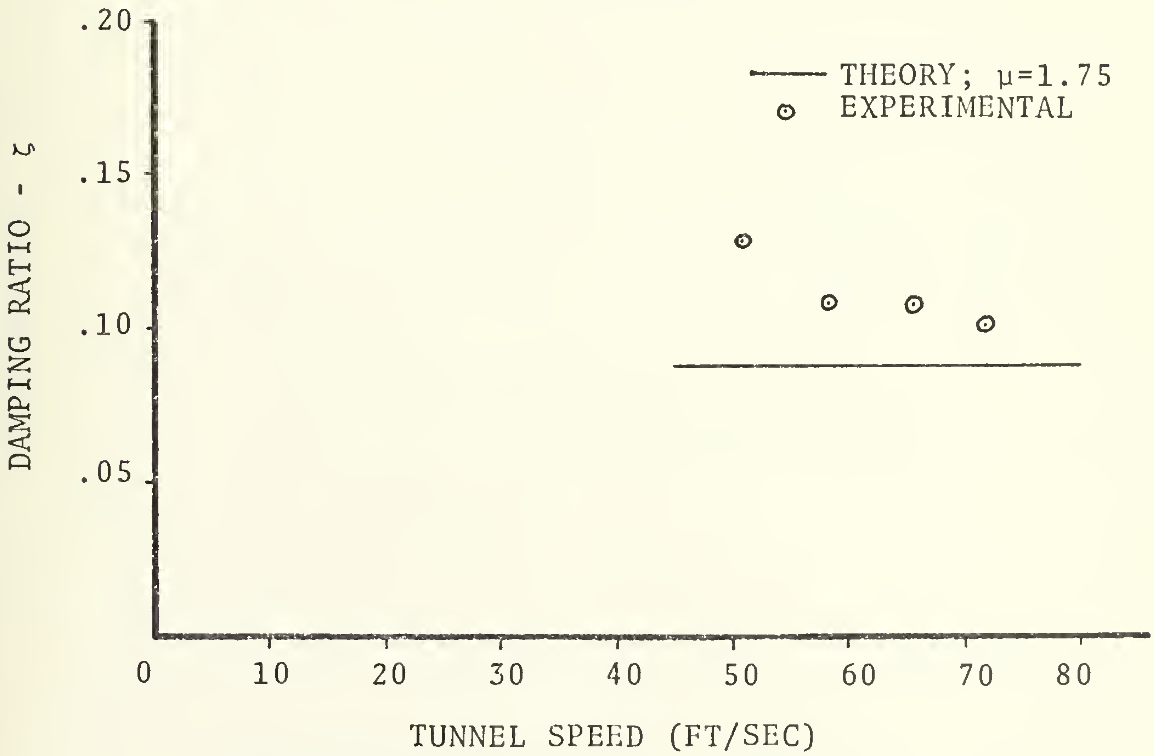

Figure V-8. Longitudinal Damping Ratio vs. Tunnel Speed

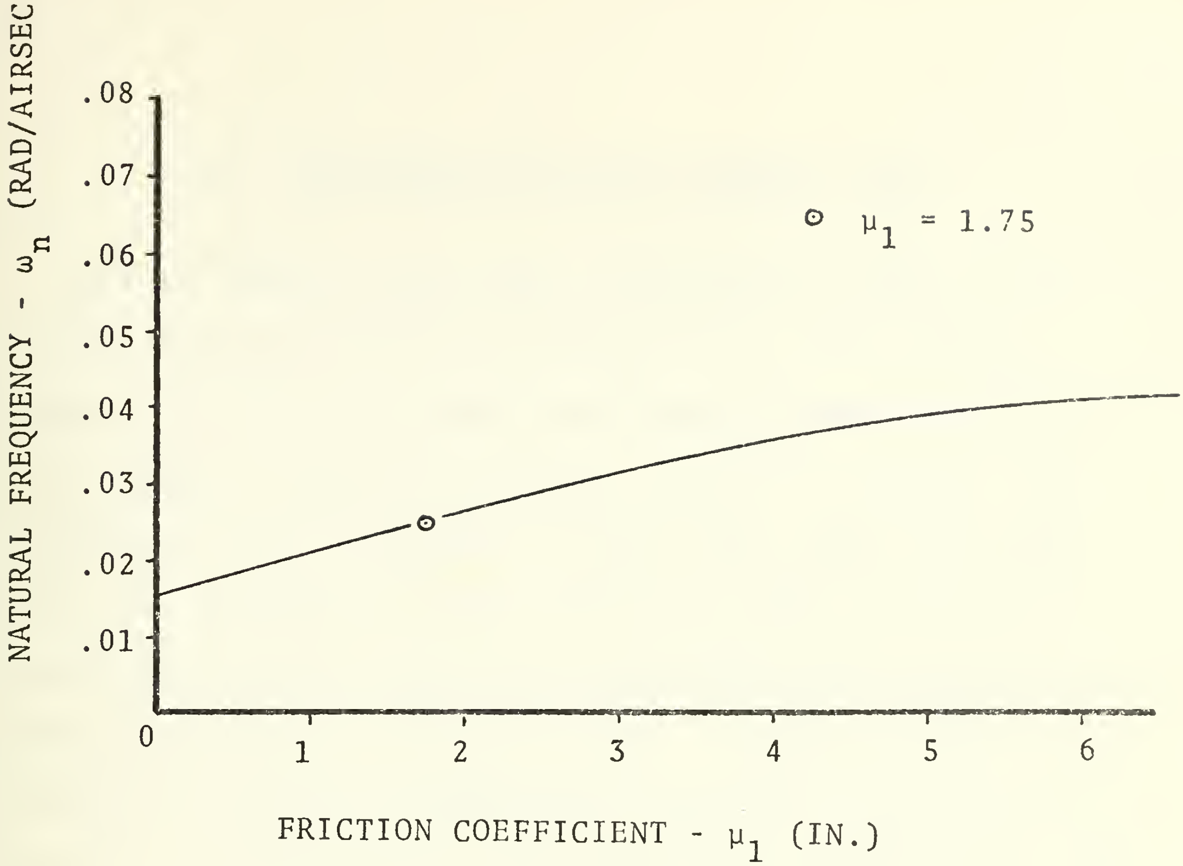

Figure V-9. Predicted Natural Frequency vs. Friction Coefficient

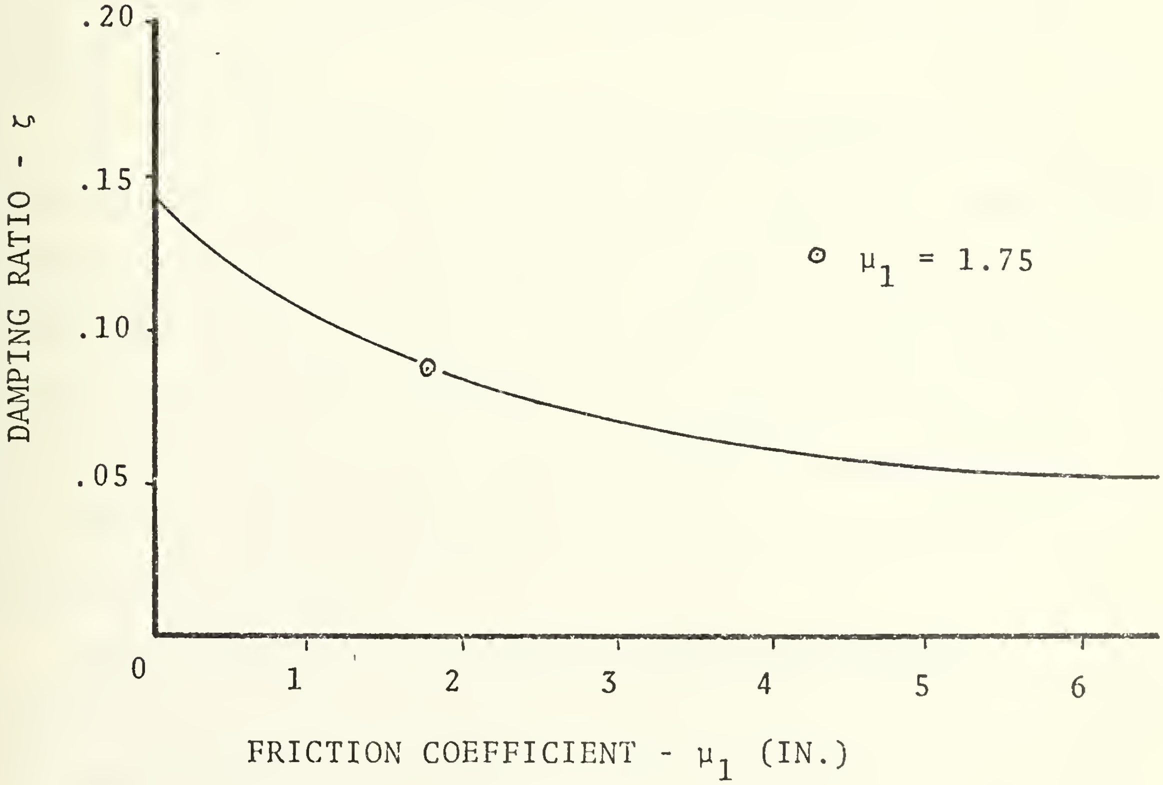

Figure V-10. Predicted Damping Ratio vs. Friction Coefficient

VI. RECOMMENDATIONS FOR FURTHER STUDY

Due to insufficient time, an extensive study of the lateral characteristics of the model was not possible. However, it must be pointed out that the model exhibited very unstable handling qualities in roll. In fact, this instability was detrimental to the point where the model had to be restrained from rolling in order to obtain the degree of accuracy required to satisfactorily determine the model longitudinal characteristics. Further study in this area of the model's response may reveal the reason for, as well as a solution for, this unpredicted instability. The model lateral response should be carefully examined and compared with the theoretical values obtained from the computer program.

The fact that there presently exist difficulties in the roll characteristics of the model should not immediately bring a conclusion that the basic concept of a three-degree-of-freedom stability and control model is impractical. Rather, with continued testing and refinement it is believed that a tool such as this will become an invaluable asset to students actively engaged in the study of aircraft stability and control.

Additionally, it is suggested that the friction coefficient of the main support bearing and yaw potentiometer be experimentally calibrated so that the model response may

be correlated more accurately. In fact, a total redesign of the main support bearing for less friction would greatly simplify and increase the accuracy of the predicted response.

APPENDIX A

LATERAL STABILITY DERIVATIVE EQUATIONS

The following equations for the lateral stability derivatives were obtained from Ref. 3, and, unless otherwise stated, any specific figures mentioned in this appendix are from that reference.

A. VARIATION OF SIDE FORCE COEFFICIENT WITH SIDESLIP ANGLE - C_{y_β}

$$C_{y_\beta} = C_{y_{\beta_W}} + C_{y_{\beta_B}} + C_{y_{\beta_V}} \qquad \text{A-1}$$

The wing contribution to this derivative may be estimated from:

$$C_{y_{\beta_W}} = -.0001\ |\Gamma|\ 57.3 \qquad \text{A-2}$$

where Γ is the wing goemetric dihedral in degrees.

The body contribution may be found by using:

$$C_{y_{\beta_B}} = -2\ K_i\ \left(\frac{S_o}{S}\right) \qquad \text{A-3}$$

where: K_i = a wing-body interference factor obtained from Fig. 7.1

S_o = the cross sectional area of the fuselage at the point along the body where the flow ceases to be potential.

S = the aircraft reference area.

The vertical tail contribution may be estimated using:

$$C_{y_{\beta_V}} = -k\, C_{L_{\alpha_V}} \left(1 + \frac{d\sigma}{d\beta}\right) n_V \frac{S_V}{X} \qquad \text{A-4}$$

where: k = an empirical factor defined in Fig. 7.3

$C_{L_{\alpha_V}}$ = vertical tail lift curve slope

$$\left(1 + \frac{d\sigma}{d\beta}\right) n_V = .724 + 3.06 \frac{S_V/S}{1 + \cos\Lambda c/4} + .4 \frac{Z_w}{d} + .009\, A$$

S_V = vertical tail area

S = reference area

A = aspect ratio

Z_w = vertical distance from the wing root quarter chord to the fuselage centerline (positive for wing above centerline)

d = fuselage diameter at wing intersection

B. VARIATION OF ROLLING MOMENT COEFFICIENT WITH SIDESLIP ANGLE - C_{1_β}

$$C_{1_\beta} = C_{1_{\beta_{WB}}} + C_{1_{\beta_H}} + C_{1_{\beta_V}} \qquad \text{A-5}$$

The wing-body contribution may be determined from:

$$C_{l_{\beta_{WB}}} = 57.3 \left\{ C_{L_{WB}} \left[\left(\frac{C_{l_\beta}}{C_L}\right)_{\Lambda c/2} K_{M_\Lambda} K_f + \left(\frac{C_{l_\beta}}{C_L}\right)_A \right] + \Gamma \left[\frac{C_{l}}{\Gamma} K_{M_\Gamma} + \frac{\Delta C_{l_\beta}}{\Gamma} \right] + (\Delta C_{l_\beta})_{Z_w} \right\} \qquad \text{A-6}$$

where: $C_{L_{WB}}$ = wing-body lift coefficient

$\left(\frac{C_{l_\beta}}{C_L}\right)_{\Lambda c/2}$ = wing sweep contribution obtained from Fig. 7.11

K_{M_Λ} = the compressibility correction to sweep from Fig. 7.12

K_f = the fuselage correction factor from Fig. 7.13

$\left(\frac{C_{l_\beta}}{C_L}\right)_A$ = contribution from aspect ratio obtained from Fig. 7.14

Γ = dihedral angle

$\frac{C_{l_\beta}}{\Gamma}$ = dihedral effect of the wing from Fig. 7.15

K_{M_Γ} = compressibility correction to dihedral from Fig. 7.16

$\frac{\Delta C_{l_\beta}}{\Gamma} = -.0005\, A \left(\frac{d}{b}\right)^2$

b = wing span

d = diameter of fuselage at wing intersection

$(\Delta C_{l_\beta})_{Z_w} = \frac{1.2\, A}{57.3} \left(\frac{Z_w}{b}\right) \left(\frac{2d}{b}\right)$

Z_w was previously defined for equation A-4.

The horizontal tail contribution is given as:

$$C_{l_{\beta_H}} = C_{l_{\beta_{HB}}} \frac{S_H}{S} \frac{b_H}{b} \qquad \text{A-7}$$

where: S_H = horizontal tail area

b_H = horizontal tail span

$C_{l_{\beta_{WB}}}$ is obtained by solving equation A-6 using the horizontal tail characteristics vice the wing.

The vertical tail contribution is given by:

$$C_{l_{\beta_V}} = C_{y_{\beta_V}} \frac{(Z_v \cos \alpha - l_v \sin \alpha)}{b} \qquad \text{A-8}$$

where: $C_{y_{\beta_V}}$ was previously determined using equation A-4

α = angle of attack of the wing

Z_v = absolute distance from fuselage centerline to vertical tail aerodynamic center (a.c.)

l_v = absolute distance from model c.g. to vertical tail a.c.

C. VARIATION OF YAWING MOMENT COEFFICIENT WITH SIDESLIP ANGLE - C_{n_β}

$$C_{n_\beta} = C_{n_{\beta_B}} + C_{n_{\beta_V}} \qquad \text{A-9}$$

The body contribution to equation A-9 is given by:

$$C_{n_{\beta_B}} = -57.3\ K_N\ K_{R_1}\ \frac{S_{B_S}}{S}\ \frac{l_B}{b} \qquad \text{A-10}$$

where: K_N = an empirical factor for body and wing-body effects from Fig. 7.19.

K_{R_1} = Reynolds Number factor for the fuselage from Fig. 7.20

S_{B_S} = body side area

l_B = overall fuselage length

The vertical tail contribution is:

$$C_{n_{\beta_V}} = -C_{y_{\beta_V}} \frac{(l_v \cos \alpha + Z_v \sin \alpha)}{b} \qquad \text{A-11}$$

where all the elements have been previously defined.

D. VARIATION OF ROLLING MOMENT COEFFICIENT WITH ROLL RATE - C_{l_p}

$$C_{l_p} = C_{l_{p_{WB}}} + C_{l_{p_H}} + C_{l_{p_V}} \qquad \text{A-12}$$

The wing-body contribution to the above equation is:

$$C_{l_{p_{WB}}} \simeq C_{l_{p_W}} = \left(\frac{\beta C_{l_p}}{k}\right) \frac{k}{\beta} \qquad \text{A-13}$$

where: $\left(\frac{\beta C_{l_p}}{k}\right)$ = roll damping parameter from Fig. 8.1

k = the ratio of the average wing section lift curve slope $C_{l_{\alpha_W}}$ to 2π

$$\beta = \sqrt{1-M^2}$$

The horizontal tail contribution is:

$$C_{l_{p_H}} = .5\ (C_{l_p})_H \frac{S_H}{S} \left(\frac{b_H}{b}\right)^2 \qquad \text{A-14}$$

where: $(C_{l_p})_H$ is obtained by solving equation A-13 for the horizontal tail.

The vertical contribution is estimated using:

$$C_{l_{p_V}} = 2 \left(\frac{Z_V}{b}\right)^2 C_{y_{\beta_V}} \qquad \text{A-15}$$

where all the variables have been previously defined in this appendix.

E. VARIATION OF YAWING MOMENT COEFFICIENT WITH ROLL RATE - C_{n_p}

$$C_{n_p} = C_{n_{p_W}} + C_{n_{p_V}} \qquad \text{A-16}$$

The wing contribution is estimated using the following equation.

$$C_{n_{p_W}} = -C_{l_{p_W}} \tan\alpha - \left[-C_{l_p} \tan\alpha - \left(\frac{C_{n_p}}{C_L}\right)_{\substack{C_L=0\\ M}} C_L\right] \qquad \text{A-17}$$

where:

$C_{l_{p_W}}$ is found from equation A-13

α = wing angle of attack

C_L = wing lift coefficient

$$\left(\frac{C_{n_p}}{C_L}\right)_{\substack{C_L=0\\ M}} = \left(\frac{A+4\cos\Lambda_{c/4}}{AB+4\cos\Lambda_{c/4}}\right) \frac{AB+\frac{1}{2}(AB+\cos\Lambda_{c/4})\tan^2\Lambda_{c/4}}{A+\frac{1}{2}(A+\cos\Lambda_{c/4})\tan^2\Lambda_{c/4}} \left(\frac{C_{n_p}}{C_L}\right)_{\substack{C_L=0\\ M=0}} \qquad \text{A-18}$$

A = aspect ratio

$B = \sqrt{1-M^2\cos^2\Lambda_{c/4}}$

M = mach number

$$\left(\frac{C_{n_p}}{C_L}\right)_{\substack{C_L=0\\ M=0}} = -\frac{1}{6}\,\frac{A+6(A+\cos\Lambda_{c/4})\left(\frac{x}{\bar{c}}\,\frac{\tan\Lambda_{c/4}}{A} + \frac{\tan^2\Lambda_{c/4}}{12}\right)}{A+4\cos\Lambda_{c/4}} \qquad \text{A-19}$$

The vertical tail contribution may be found from:

$$C_{n_{p_V}} = -\frac{2}{b}\,(l_V\cos\alpha + Z_V\sin\alpha)\left(\frac{Z_V\cos\alpha - l_V\sin\alpha - Z_V}{b}\right) C_{y_{\beta_V}} \qquad \text{A-20}$$

where all the elements of A-20 have been previously defined.

F. VARIATION OF ROLLING MOMENT COEFFICIENT WITH YAW RATE - C_{l_r}

$$C_{l_r} = C_{l_{r_W}} + C_{l_{r_V}} \qquad \text{A-21}$$

The wing contribution is given by:

$$C_{l_{r_W}} = C_L \left(\frac{C_{l_r}}{C_L}\right)_{\substack{C_L=0\\ M}} + \left(\frac{\Delta C_{l_r}}{\Gamma}\right) \qquad \text{A-22}$$

where: C_L = wing lift coefficient

$$\left(\frac{C_{l_r}}{C_l}\right)_{\substack{C_L=0\\ M}} = \frac{1 + \frac{A(1-B^2)}{2B(AB+2\cos\Lambda_{c/4})} + \frac{AB+2\cos\Lambda_{c/4}}{AB+4\cos\Lambda_{c/4}}\ \frac{\tan^2\Lambda_{c/4}}{8}}{1 + \frac{A+2\cos\Lambda_{c/4}}{A+4\cos\Lambda_{c/4}}\ \frac{\tan^2\Lambda_{c/4}}{8}} \left(\frac{C_{l_r}}{C_L}\right)_{\substack{C_L=0\\ M=0}} \qquad \text{A-23}$$

$\left(\frac{C_{l_r}}{C_L}\right)_{\substack{C_L=0\\ M=0}}$ is obtained from Fig. 9.1

$$\frac{\Delta C_{l_r}}{\Gamma} = \frac{1}{12}\ \frac{A\sin\Lambda_{c/4}}{A+4\cos\Lambda_{c/4}}$$

Γ = wing dihedral angle in radians.

The vertical tail contribution is found from:

$$C_{l_{r_V}} = \frac{-2}{b^2}(l_V \cos\alpha + Z_V \sin\alpha)(Z_V \cos\alpha - l_V \sin\alpha)\, C_{y_{\beta_V}} \qquad \text{A-24}$$

where all the variables have been previously defined.

G. VARIATION OF YAWING MOMENT COEFFICIENT WITH YAW RATE - C_{n_r}

$$C_{n_r} = C_{n_{r_W}} + C_{n_{r_V}} \qquad \text{A-25}$$

The wing contribution is found from:

$$C_{n_{r_W}} = \left(\frac{C_{n_r}}{C_L^2}\right) C_L^2 + \left(\frac{C_{n_r}}{C_{D_o}}\right) C_{D_o} \qquad \text{A-26}$$

where:

$\left(\frac{C_{n_r}}{C_L^2}\right)$ is found from Fig. 9.4.

$\left(\frac{C_{n_r}}{C_{D_o}}\right)$ is found from Fig. 9.5.

C_{D_o} is the model zero-lift drag coefficient.

The vertical tail contribution may be estimated from:

$$C_{n_{r_V}} = \frac{2}{b^2}(l_V \cos\alpha + Z_V \sin\alpha)^2\, C_{y_{\beta_V}} \qquad \text{A-27}$$

where all the variables have been previously determined.

H. VARIATION OF ROLLING MOMENT COEFFICIENT WITH AILERON DEFLECTION - C_{l_ξ}

The procedure for determining this coefficient is a rather complex step-by-step process highly dependent upon the exact type of aileron employed. Therefore, it is suggested that Ref. 3 be consulted for the determination of this derivative.

I. VARIATION OF YAWING MOMENT COEFFICIENT WITH AILERON DEFLECTION - C_{n_ξ}

$$C_{n_\xi} = K \, C_L \, C_{l_\xi} \tag{A-28}$$

where: K = an empirical factor obtained from Fig. 11.3

C_L = the model steady state lift coefficient

C_{l_ξ} = the derivative determined in section H

J. VARIATION OF ROLLING MOMENT COEFFICIENT WITH RUDDER DEFLECTION - $C_{l_{\delta_F}}$

Reference 1 was used to determine the value of this derivative. The following equation was used.

$$C_{l_{\delta_F}} = C_{L_{\alpha_V}} \frac{S_V}{S} \frac{Z_v}{b} \tag{A-29}$$

where: $C_{L_{\alpha_V}}$ = vertical tail lift curve slope

S_V = vertical tail area

K. VARIATION OF YAWING MOMENT COEFFICIENT WITH RUDDER DEFLECTION - $C_{n_{\delta_F}}$

Reference 1 was used to determine the value of this derivative also. The following equation was used:

$$C_{n_{\delta_F}} = C_{L_{\alpha_V}} \frac{S_V}{S} \frac{l_v}{b} \qquad \text{A-30}$$

where all the variables are known.

```
**************************************************************
**************************************************************
**                                                          **
**                                                          **
**                 MODEL CHARACTERISTICS                    **
**                                                          **
**                                                          **
**************************************************************
**************************************************************
```

TOTAL MODEL PARAMETERS:

```
TRIM LIFT COEFFICIENT (CL) =         0.0

MODEL ANGLE OF ATTACK (DEG.) = -5.0982669D-01

TAIL ANGLE OF ATTACK (DEG) =         2.4765951D 00

TOTAL LENGTH (IN) =                  2.9000000D 01

TOTAL WEIGHT (LBS) =                 4.6997845D 00

STICK FIXED STATIC MARGIN =          2.2599784D-01

LIFT CURVE SLOPE (PER RAD.) =        5.0624000D 00


              MOMENTS OF INERTIA (IN2-LBS)

I(X) =   6.2023497D 01        I(Y) =    2.6436234D 02

I(Z) =   3.1432216D 02        I(XZ) =   1.0348581D 01


MODEL C.G. WITH RESPECT TO REFERENCE AXIS ORIGIN (IN)

XBAR =   4.7068655D-02        YBAR =  -3.1916357D-03

ZBAR =  -1.6414961D-02
```

WING AND TAIL SURFACE PARAMETERS:

-WING CHARACTERISTICS-

ROOT CHORD (IN) =	6.1500000D 00
TIP CHORD (IN) =	1.8500000D 00
WING SPAN (IN) =	3.0000000D 01
WING AREA (IN2) =	1.2000000D 02
L.E. SWEEP (DEG) =	2.3500000D 01
DIHEDRAL ANGLE (DEG) =	6.0000000D 00
LIFT CURVE SLOPE (PER RAD) =	4.5309000D 00

-HORIZONTAL TAIL CHARACTERISTICS-

ROOT CHORD (IN) =	3.9375000D 00
TIP CHORD (IN) =	9.3000000D-01
TAIL SPAN (IN) =	1.3125000D 01
TAIL AREA (IN2) =	3.1100000D 01
L.E. SWEEP (DEG) =	2.5200000D 01
DIHEDRAL ANGLE (DEG) =	0.0
LIFT CURVE SLOPE (PER RAD) =	4.0211000D 00

-VERTICAL TAIL CHARACTERISTICS-

ROOT CHORD (IN) =	6.5000000D 00
TIP CHORD (IN) =	1.5000000D 00
TAIL HEIGHT (IN) =	6.3750000D 00
TAIL AREA (IN2) =	2.6000000D 01
L.E. SWEEP (DEG) =	5.0000000D 01
LIFT CURVE SLOPE (PER RAD) =	2.9891000D 00

LONGITUDINAL STABILITY DERIVATIVES:

CM- = VARIATION OF PITCHING MOMENT COEFFICIENT
WITH -
A = ANGLE OF ATTACK (ALFA)   Q = PITCH RATE
A(DOT) = VARIATION OF ALFA WITH RESPECT TO TIME

CMQ =	-1.4979070D 01	CMA =	-1.1440915D 00
CMA(DOT) =	-6.2308383D 00	CMA(TAIL) =	-2.9448839D 00

ELEMENTS OF STATE VARIABLE MATRIX A ARE:

-4.4970234D-03	-2.4257559D-04
1.0000000D 00	0.0

ELEMENTS OF THE B VECTOR ARE:

-6.2438798D-04
0.0

LATERAL STABILITY DERIVATIVES:

CL- = VARIATION OF ROLLING MOMENT COEFFICIENT
WITH -

CN- = VARIATION OF YAWING MOMENT COEFFICIENT
WITH -

B = SIDESLIP ANGLE (BETA)

P = ROLL RATE   R = YAW RATE

DA = AILERON DEFLECTION   DF = RUDDER DEFLECTION

CLB = -1.2537315D-01	CNB = 7.3790651D-02
CLP = -4.3806752D-01	CNP = -2.5131716D-03
CLR = 4.3663509D-02	CNR = -1.5384192D-01
CLDA = 6.9936720D-01	CNDA = -1.1977032D-03
CLDF = 5.5541463D-02	CNDF = -2.3746739D-01

ELEMENTS OF STATE VARIABLE MATRIX A ARE:

-1.2747884D-01	1.1230146D-02	-3.5770197D-02	0.0
-4.3405394D-03	-8.4139888D-03	3.0354552D-03	0.0
0.0	-1.0000000D 00	0.0	0.0
1.0000000D 00	0.0	0.0	0.0

ELEMENTS OF THE B MATRIX ARE:

2.0346785D-01	1.3884961D-02
6.6304872D-03	-1.3101244D-02
0.0	0.0
0.0	0.0

```
     THIS PROGRAM COMPUTES THE MODEL LONGITUDINAL AND LATERAL STABILITY
DERIVATIVES AS WELL AS THE MOMENTS OF INERTIA.  IT THEN USES THESE VALUES
TO DETERMINE THE ELEMENTS OF THE 'A' AND 'B' MATRICIES, FOR THE FRICTIONLESS
CASE, WHICH ARE USED IN THE STATE REPRESENTATION OF THE EQUATIONS OF MOTION.

     UNLESS OTHERWISE STATED, ALL LENGTH QUANTITIES ARE IN UNITS OF INCHES
AND ALL AREA QUANTITIES ARE IN UNITS OF SQUARE INCHES.  ALL FIGURES REFERED
TO IN THE SECTION DESCRIBING THE REQUIRED INPUT CARDS MAY BE FOUND IN REF. 3
OF THIS THESIS.  THIS PROGRAM IS NOT APPLICABLE FOR A MODEL HAVING A WING
WITH GEOMETRIC TWIST AND SHOULD NOT BE USED IN SUCH A CASE.

     UNLESS OTHERWISE SPECIFIED, ALL INPUT CARDS ARE OF THE FORMAT XF10.7,
WHERE 'X' IS THE NUMBER OF REAL CONSTANTS TO BE PUNCHED IN EACH CARD.  A
DESCRIPTION OF THE INPUT QUNATITIES REQUIRED FOR THIS PROGRAM FOLLOWS.

                    ****************************************


  CARD # 1:
    COL. 1) FL - OVERALL FUSELAGE LENGTH
        11) CN - ABSOLUTE DISTANCE FROM NOSE OF FUSELAGE TO C.G.
        21)  T - FUSELAGE SKIN THICKNESS

  CARD # 2:
    COL. 1) DENSK - DENSITY OF SKIN MATERIAL (LB/FT**3)
        11) DENW  - DENSITY OF WING MATERAL (LB/FT**3)
        21) DENT  - DENSITY OF HORIZONTAL TAIL MATERIAL (LB/FT**3)
        31) DENV  - DENSITY OF VERTICAL TAIL MATERIAL (LB/FT**3)

  CARD # 3:
    COL. 1) D(1) - INSIDE DIAMETER OF FUSELAGE AT NOSE

  CARD # 4:
    COL. 1) D(2) - INSIDE DIAMETER OF FUSELAGE AT (FL)/20 IN. AFT OF THE NOSE

  CARD # 5:
    COL. 1) D(3) - INSIDE DIAMETER OF FUSELAGE AT (2*FL)/20 IN. AFT OF THE NOSE

     "        "        "        "        "        "        "        "
```

```
  "          "          "          "          "          "          "          "

CARD # (Y+2):
  COL. 1) D(Y) - INSIDE DIAMETER OF FUSELAGE AT (Y-1)*FL/20 IN AFT OF NOSE

  "          "          "          "          "          "          "          "

  "          "          "          "          "          "          "          "

CARD #23:
  COL. 1) D(21) - INSIDE DIAMETER AT THE TAIL OF THE FUSELAGE

CARD #24:
  COL. 1) RT - AVERAGE THICKNESS OF MAIN WING AT THE FUSELAGE
      11) TT - AVERAGE THICKNESS OF MAIN WING AT TIP
      21) CT - WING TIP CHORD
      31) CR - WING CHORD AT FUSELAGE
      41) CR1- WING ROOT CHORD

CARD #25:
  COL. 1) RMPT - LOCATION ALONG THE X-AXIS OF THE MIDPOINT OF THE WING CHORD
                 AT THE FUSELAGE JUNCTION (NEGATIVE IF AFT OF C.G.)
      11) TMPT - LOCATION ALONG X-AXIS OF WING TIP CHORD MIDPOINT (NEG. IF
                 AFT OF C.G.)
      21) WS   - LENGTH OF EXPOSED WING SEMI-SPAN
      31) DISTW- LENGTH OF WING SEMI-SPAN COVERED BY FUSELAGE

CARD #26:
  COL. 1) GAMAW - DIHEDRAL ANGLE OF THE WING (DEG)
      11) SWLEW - LEADING EDGE SWEEP OF THE WING (DEG)

CARD #27:
  COL. 1) CRT  - CHORD OF THE HORIZONTAL TAIL AT THE FUSELAGE
      11) CTT  - HORIZONTAL TAIL TIP CHORD
      21) TRT  - AVERAGE THICKNESS OF THE HORIZONTAL TAIL AT THE FUSELAGE
      31) TTT  - AVERAGE THICKNESS OF THE HORIZONTAL TAIL AT THE TIP
      41) CRT1- HORIZONTAL TAIL ROOT CHORD
```

```
CARD #28:
  COL. 1) DIST - LENGTH OF HORIZ. TAIL SEMI-SPAN COVERED BY THE FUSELAGE
      11) TMPTR- LOCATION ALONG X-AXIS OF THE MIDPT. OF THE HORIZ. TAIL CHORD
                 AT THE FUSELAGE INTERSECTION (NEG. IF AFT OF C.G.)
      21) TMPTT- LOCATION ALONG X-AXIS OF HORIZ. TAIL TIP CHORD MIDPT.


CARD #29:
  COL. 1) GAMAT - HORIZ. TAIL DIHEDRAL ANGLE (DEG.)
      11) TS    - LENGTH OF EXPOSED HORIZ. TAIL SEMI-SPAN
      21) SWLET - HORIZ. TAIL LEADING EDGE SWEEP (DEG)


CARD #30:
  COL. 1) VRC - CHORD OF VERTICAL TAIL AT THE FUSELAGE
      11) VTC - VERT. TAIL TIP CHORD
      21) VRT - AVERAGE THICKNESS OF VERT. TAIL CHORD AT FUSELAGE
      31) VTT - AVERAGE THICKNESS OF VERT. TAIL CHORD AT TIP
      41) VRC1- VERT. TAIL ROOT CHORD


CARD #31:
  COL. 1) VDIS  - PORTION OF THE TAIL HEIGHT COVERED BY FUSELAGE
      11) VMPTR- LOCATION ALONG X-AXIS OF THE MIDPT. OF THE VERT. TAIL CHORD
                 AT THE FUSELAGE INTERSECTION (NEG. IF AFT OF C.G.)
      21) VMPTT- LOCATION ALONG X AXIS OF VERT. TAIL TIP CHORD MIDPT.
      31) VB    - EXPOSED VERTICAL TAIL HEIGHT


CARD #32:
  COL. 1) VS    - VERT. TAIL AREA INCLUDING PORTION COVERED BY FUSELAGE
      11) CLAV  - VERT. TAIL LIFT CURVE SLOPE (PER RAD.)
      21) SWLEV- VERT. TAIL LEADING EDGE SWEEP (DEG)


CARD #33:   ***NOTE: FORMAT I2***
  COL. 1&2) N -  NUMBER OF INTERNAL LUMPED MASSES (AN INTEGER)


CARD #34A:
  COL. 1) W - THE WEIGHT OF THE FIRST LUMPED MASS (LBS.)
      11) X - THE X LOCATION OF THE PARTICULAR MASS
      21) Y - THE Y LOCATION OF THE MASS
      31) Z - THE Z LOCATION OF THE MASS


CARD #34B:
  COL. 1) W - THE WEIGHT OF THE SECOND MASS (LBS.)
```

```
        11) X - THE X LOCATION OF THE SECOND MASS
        21) Y - THE Y LOCATION OF THE SECOND MASS
        31) Z - THE Z LOCATION OF THE SECOND MASS

   "         "         "         "         "

   "         "         "         "         "

CARD #34N:
  COL. 1) W - THE WEIGHT OF THE NTH MASS (LBS.)
      11) X - THE X LOCATION OF THE NTH MASS
      21) Y - THE Y LOCATION OF THE NTH MASS
      31) Z - THE Z LOCATION OF THE NTH MASS

CARD #35:  PUT * IN THE FIRST 20 COLS.

CARD #36:
  COL. 1) H    - C.G. POSITION, FRACTION OF M.A.C.
      11) CLTRM- DESIRED TRIM LIFT COEFFICIENT

CARD #37:
COL. 1) ST - HORIZ. TAIL AREA INCLUDING PORTION COVERED BY FUSELAGE

CARD #38:
  COL. 1) TL    - ABSOLUTE DISTANCE FROM C.G. TO HORIZ. TAIL A.C.
      11) TH    - VERT. DISTANCE BETWEEN HORIZ. TAIL ROOT CHORD AND FUSELAGE
                  CENTERLINE (POSITIVE FOR TAIL BELOW CENTERLINE)
      21) CLAT  - HORIZ. TAIL LIFT CURVE SLOPE (PER RAD.)
      31) CMOWB- ZERO LIFT PITCHING MOMENT OF THE WING-BODY COMBINATION

CARD #39:
  COL. 1) WA    - WING AREA INCLUDING PORTION COVERED BY FUSELAGE
      11) WB    - WING SPAN
      21) HNWB  - NEUTRAL POINT OF WING-BODY COMBINATION, FRACTION OF M.A.C.
      31) SWLEW- WING LEADING EDGE SWEEP (DEG.)

CARD #40:
  COL. 1) CR1   - WING ROOT CHORD
      11) CT    - WING TIP CHORD
```

```
      21) GAMAW- WING DIHEDRAL ANGLE (DEG.)
      31) ALFAZL- WING ANGLE OF ATTACK FOR ZERO LIFT (DEG.)


CARD #41:
  COL. 1) CLAW - WING LIFT CURVE SLOPE (PER RAD.)
      11) CLAWS- WING SECTION LIFT CURVE SLOPE (PER RAD.)
      21) CLAM - MODEL LIFT CURVE SLOPE (PER RAD.)
      31) CLAWB- WING-BODY LIFT CURVE SLOPE (PER RAD.)


CARD #42:
  COL. 1) CLBCLS - WING SWEEP CONTRIBUTION OF VARIATION OF ROLLING MOMENT
                   COEFFICIENT WITH SIDESLIP ANGLE, OBTAINED FROM FIG. 7.11
                   OF REF. 3
      11) SKM    - COMPRESSIBILITY CORRECTION TO SWEEP OBTAINED FROM FIG. 7.12
      21) FK     - FUSELAGE CORRECTION FACTOR OBTAINED FROM FIG. 7.13
      31) CLBCLA - ASPECT RATIO CONTRIBUTION FROM FIG. 7.14
      41) CLBG   - WING DIHEDRAL EFFECT FROM FIG. 7.15
      51) GKM    - COMPRESSIBILITY CORRECTION TO DIHEDRAL FROM FIG. 7.16


CARD #43:
  COL. 1) H  - C.G. POSITION, FRACTION OF M.A.C.
      11) ZW - VERT. DISTANCE FROM WING ROOT TO FUSELAGE CENTERLINE (POSITIVE
               FOR WING ROOT BELOW CENTERLINE)


CARD #44:
  COL. 1) HCBCLS - ..
      11) HSKM   -  ..
      21) HFK    -  ...  SAME CONSTANTS AS DESCRIBED IN CARD #42 BUT
      31) HCBCLA -  ...  EVALUATED FOR THE HORIZONTAL TAIL
      41) HCLBG  -  ..
      51) HGKM   - ..


CARD #45:
  COL. 1) ZWH - VERT. DISTANCE FROM HORIZ. TAIL ROOT TO FUSELAGE CENTERLINE
                (POSITIVE FOR TAIL ROOT BELOW CENTERLINE)


CARD #46:
  COL. 1) CONSTV - EMPIRICAL FACTOR FOR ESTIMATING THE CONTRIBUTION TO
                   SIDESLIP FOR SINGLE VERT. TAIL FROM FIG. 7.3
      11) CLAV   - VERT. TAIL LIFT CURVE SLOPE (PER RAD.)
      21) VS     - VERT. TAIL AREA INCLUDING PORTION COVERED BY FUSELAGE
```

```
CARD #47:
  COL. 1) ZV - ABSOLUTE DISTANCE FROM FUSELAGE CENTERLINE TO VERT. TAIL A.C.
      11) VL - ABSOLUTE DISTANCE FROM C.G. TO VERT. TAIL A.C.

CARD #48:
  COL. 1) XKN    - WING-BODY INTERFERENCE FACTOR FROM FIG. 7.19
      11) XKRL   - EFFECT OF FUSELAGE REYNOLDS NUMBER FROM FIG. 7.20
      21) SBS    - BODY SIDE AREA
      31) FL     - TOTAL FUSELAGE LENGTH

CARD #49:
  COL. 1) XBCLPK - ROLL DAMPING PARAMETER FROM FIG. 8.1
      11) CLAWS  - WING SECTION LIFT CURVE SLOPE (PER RAD.)
      21) HBCLPK - ROLL DAMPING PARAMETER FOR HORIZONTAL TAIL FROM FIG. 8.1
      31) CLATS  - LIFT CURVE SLOPE OF HORIZONTAL TAIL SECTION (PER RAD.)

CARD #50:
  COL. 1) XBAR1 - DISTANCE FROM MODEL C.G. TO MODEL A.C. (POSITIVE WHEN
                  A.C. IS AFT OF C.G.)

CARD #51:
  COL. 1) XCLRCL - SLOPE OF THE LOW SPEED ROLLING MOMENT DUE TO YAWING
                   AT ZERO LIFT OBTAINED FROM FIG. 9.1

CARD #52:
  COL. 1) XCNRCL - LOW SPEED DRAG DUE TO LIFT YAW-DAMPING PARAMETER OBTAINED
                   FROM FIG. 9.4
      11) XCNRCD - LOW SPEED PROFILE DRAG YAW-DAMPING PARAMETER FROM FIG. 9.5
      21) CDO    - ZERO-LIFT DRAG COEFFICIENT OF THE MODEL

CARD #53:
  COL. 1) BCPLDK - AILERON ROLLING MOMENT PARAMETER FROM FIG. 11.1
      11) CLDTD  - EMPIRICAL CORRECTION FOR LIFT EFFECTIVENESS OF PLAIN
                   TRAILING EDGE FLAPS FROM FIG. 10.6
      21) CLDT   - LIFT EFFECTIVENESS OF PLAIN TRAILING EDGE FLAPS FROM
                   FIGURE 10.5
      31) CK     - CORRELATION CONSTANT FOR DETERMINING YAWING MOMENT DUE
                   TO AILERON DEFLECTIONS FROM FIG. 11.3

******************** THIS ENDS THE REQUIRED DATA INPUTS *********************
```

```
      IMPLICIT REAL*8(A-H,O-Z)
C
CCCCCCCCCCCCCCCCCCCCCCCCCCCCCCCCCCCCCCCCCCCCCCCCCCCCC
C                                                   C
C   COMPUTATION OF MODEL C.G. AND MOMENTS OF INERTIA  C
C                                                   C
CCCCCCCCCCCCCCCCCCCCCCCCCCCCCCCCCCCCCCCCCCCCCCCCCCCCC
C
      DIMENSION D(30), RAD(30)
      DIMENSION WM(30), XM(30), YM(30), ZM(30)
C
C   COMPUTATION OF C.G. AND MOMENTS OF INERTIA DUE TO THE FUSELAGE
C
      READ (5,170) FL,CN,T
      READ (5,160) DENSK,DENW,DENT,DENV
      WEIGHF = 0.0D0
      PRODF = 0.0D0
      PRODFV = 0.0D0
      PRODFZ = 0.0D0
      A1 = 0.0D0
      B1 = 0.0D0
      C1 = 0.0D0
      E1 = 0.0D0
      SL = FL/20.D0
      SS = SL/5.D0
      READ (5,130) D(1)
      RAD(1) = (D(1)+T)/2.D0
C
C
C
      DO 40 I=2,21
      READ (5,130) D(I)
      RAD(I) = (D(I)+T)/2.D0
      SLOPE = (RAD(I)-RAD(I-1))/SL
C
C
C
      DO 30 J=1,9,2
      SUBINT = DFLOAT(J)*SS/2.D0
      UNIT = SUBINT+(I-2)*SL
      X = CN-UNIT
      R = SUBINT*SLOPE+RAD(I-1)
      SW = R*4.D0/57.2957D0
      DELMF = SS*SW*T*DENSK/(12**3)
C
```

```
C
C
      DC 20 K=2,358,4
      ALFA = DFLOAT(K)/57.29577D0
      Z = R*DCOS(ALFA)
      Y = -R*DSIN(ALFA)
      WEIGHF = DELMF+WEIGHF
      PRODF = DELMF*X+PRODF
      PRODFV = DELMF*Y+PRODFV
      PRODFZ = DELMF*Z+PRODFZ
      A1 = DELMF*(Y**2+Z**2)+A1
      B1 = DELMF*(X**2+Z**2)+B1
      C1 = DELMF*(X**2+Y**2)+C1
      E1 = DELMF*X*Z+E1
   20 CONTINUE
C
C
C
   30 CONTINUE
C
C
C
   40 CONTINUE
C
C
C
C
C     COMPUTATION OF C.G. AND MOMENTS OF INERTIA DUE TO THE WINGS
C
      READ (5,190) RT,TT,CT,CR,CR1
      READ (5,160) RMPT,TMPT,WS,DISTW
      READ (5,150) GAMAW,SWLEW
      WEIGHW = 0.0D0
      PRODW = 0.0D0
      PRODWZ = 0.0D0
      A2 = 0.0D0
      B2 = 0.0D0
      C2 = 0.0D0
      E2 = 0.0D0
      GAMA = GAMAW/57.29577D0
      THCKR = 1.D0-TT/RT
      TAPR = 1.D0-CT/CR
      WL = WS/50.D0
      SLOPE = (TMPT-RMPT)/WS
C
C
C
      DO 50 N=1,99,2
      UNIT = DFLOAT(N)*WL/2.D0
```

```
      HYP = DISTW+UNIT
      CORD = CR*(1.DO-TAPR*UNIT/WS)
      THICK = RT*(1.DO-THCKR*UNIT/WS)
      VOLW = WL*CORD*THICK/(12**3)
      DELMW = VOLW*DENW
      X = SLOPE*UNIT+RMPT
      Y = HYP*DCOS(GAMA)
      Z = -HYP*DSIN(GAMA)
      WEIGHW = DELMW+WEIGHW
      PRODW = DELMW*X+PRODW
      PRODWZ = DELMW*Z+PRODWZ
      A2 = DELMW*(Y**2+Z**2)+A2
      B2 = DELMW*(X**2+Z**2)+B2
      C2 = DELMW*(X**2+Y**2)+C2
      E2 = DELMW*X*Z+E2
   50 CONTINUE
C
C
C
      WEIGHW = 2.DO*WEIGHW
      PRODW = 2.DO*PRODW
      PRODWZ = 2.DO*PRODWZ
      A2 = 2.DO*A2
      B2 = 2.DO*B2
      C2 = 2.DO*C2
      E2 = 2.DO*E2
C
C     COMPUTATION OF C.G. AND MOMENTS OF INERTIA DUE TO THE HORIZONTAL TAIL
C
      READ (5,190) CRT,CTT,TRT,TTT,CRT1
      READ (5,170) DIST,TMPTR,TMPTT
      READ (5,170) GAMAT,TS,SWLET
      TB = 2.DO*(DIST+TS)
      GAMAT = GAMAT/57.29577DO
      WEIGHH = 0.0DO
      PRCDH = 0.0DO
      PRODHZ = 0.0DO
      A3 = 0.0DO
      B3 = 0.0DO
      C3 = 0.0DO
      E3 = 0.0DO
      THICKR = 1.DO-TTT/TRT
      TAPR = 1.DO-CTT/CRT
      SLOPE = (TMPTT-TMPTR)/TS
      TL = TS/25.DO
C
C
C
```

```
      DC 60 N=1,49,2
      UNIT = DFLOAT(N)*TL/2.DO
      HYP = DIST+UNIT
      TCORD = CRT*(1.DO-TAPR*UNIT/TS)
      TTHIK = TRT*(1.DO-THICKR*UNIT/TS)
      VOLT = TL*TCORD*TTHIK/(12**3)
      DELMT = VOLT*DENT
      X = SLOPE*UNIT+TMPTR
      Y = HYP*DCOS(GAMAT)
      Z = -HYP*DSIN(GAMAT)
      WEIGHH = DELMT+WEIGHH
      PRODH = DELMT*X+PRODH
      PRODHZ = DELMT*Z+PRODHZ
      A3 = DELMT*(Y**2+Z**2)+A3
      B3 = DELMT*(X**2+Z**2)+B3
      C3 = DELMT*(X**2+Y**2)+C3
      E3 = DELMT*X*Z+E3
   60 CONTINUE
C
C
C
      WEIGHH = 2.DO*WEIGHH
      PRCDH = 2.DO*PRODH
      PRODHZ = 2.DO*PRODHZ
      A3 = 2.DO*A3
      B3 = 2.DO*B3
      C3 = 2.DO*C3
      E3 = 2.DO*E3
C
C  COMPUTATION OF C.G. AND MOMENTS OF INERTIA DUE TO THE VERTICLE TAIL
C
      READ (5,190) VRC,VTC,VRT,VTT,VRC1
      READ (5,160) VDIS,VMPTR,VMPTT,VB
      READ (5,170) VS,CLAV,SWLEV
      VDIS = DABS(VDIS)
      WEIGHV = 0.ODO
      PRODV = 0.ODO
      PRODVZ = 0.ODO
      A4 = 0.ODO
      B4 = 0.ODO
      C4 = 0.ODO
      E4 = 0.ODO
      THICKR = 1.DO-VTT/VRT
      TAPR = 1.DO-VTC/VRC
      SLOPE = (VMPTT-VMPTR)/VB
      VW = VB/25.DO
C
C
```

```
C
      DO 70 N=1,49,2
      UNIT = DFLOAT(N)*VW/2.D0
      X = SLOPE*UNIT+VMPTR
      Y = 0.0D0
      Z = (VDIS+UNIT)*(-1.D0)
      VCORD = VRC*(1.D0-TAPR*UNIT/VB)
      VTHIK = VRT*(1.D0-THICKR*UNIT/VB)
      VOLV = VW*VCORD*VTHIK/(12**3)
      DELMV = VOLV*DENV
      WEIGHV = DELMV+WEIGHV
      PRODV = DELMV*X+PRODV
      PRODVZ = DELMV*Z+PRODVZ
      A4 = DELMV*(Y**2+Z**2)+A4
      B4 = DELMV*(X**2+Z**2)+B4
      C4 = DELMV*(X**2+Y**2)+C4
      E4 = DELMV*X*Z+E4
   70 CONTINUE
C
C
C
      VB1 = VB+VDIS
C
C   COMPUTATION OF C.G. AND MOMENTS OF INERTIA DUE TO ANY LUMPED MASSES
C
      READ (5,140) N
      WEIGHM = 0.0D0
      PRODM = 0.0D0
      PRODMV = 0.0D0
      PRODMZ = 0.0D0
      A5 = 0.0D0
      B5 = 0.0D0
      C5 = 0.0D0
      E5 = 0.0D0
C
C
C
      DO 80 I=1,N
      READ (5,160) W,X,Y,Z
      WM(I) = W
      XM(I) = X
      YM(I) = Y
      ZM(I) = Z
      WEIGHM = W+WEIGHM
      PRODM = W*X+PRODM
      PRODMV = W*Y+PRODMV
      PRODMZ = W*Z+PRODMZ
      A5 = W*(Y**2+Z**2)+A5
```

```
      B5 = W*(X**2+Z**2)+B5
      C5 = W*(X**2+Y**2)+C5
      E5 = W*X*Z+E5
   80 CONTINUE
C
C
C
      WEIGHT = WEIGHF+WEIGHW+WEIGHH+WEIGHV+WEIGHM
      PRODCT = PRODF+PRODW+PRODH+PRODV+PRODM
      PRODVC = PRODFV+PRODMV
      PRODCZ = PRODFZ+PRODWZ+PRODHZ+PRODVZ+PRODMZ
      A = A1+A2+A3+A4+A5
      B = B1+B2+B3+B4+B5
      C = C1+C2+C3+C4+C5
      E = E1+E2+E3+E4+E5
      XBAR = PRODCT/WEIGHT
      YBAR = PRODVC/WEIGHT
      ZBAR = PRODCZ/WEIGHT
      WRITE (6,200)
      WRITE (6,210)
      WRITE (6,230)
      WRITE (6,230)
      WRITE (6,240)
      WRITE (6,230)
      WRITE (6,230)
      WRITE (6,210)
      WRITE (6,220)
      WRITE (6,250)
      WRITE (6,260)
      GO TO 100
   90 WRITE (6,270) CLTRM
      WRITE (6,280) ALFAW1
      WRITE (6,290) ALFAT1
      WRITE (6,300) FL
      WRITE (6,310) WEIGHT
      WRITE (6,320) SFSM
      WRITE (6,330) CLAM
      WRITE (6,340)
      WRITE (6,350) A,B
      WRITE (6,360) C,E
      WRITE (6,370)
      WRITE (6,380) XBAR,YBAR
      WRITE (6,390) ZBAR
      WRITE (6,400)
      WRITE (6,410)
      WRITE (6,420)
      WRITE (6,430) CR1
      WRITE (6,440) CT
```

```
      WRITE (6,450) WB
      WRITE (6,460) WA
      WRITE (6,470) SWLEW
      WRITE (6,480) GAMAW
      WRITE (6,490) CLAW
      WRITE (6,500)
      WRITE (6,430) CRT1
      WRITE (6,440) CTT
      WRITE (6,510) TB
      WRITE (6,520) ST
      WRITE (6,470) SWLET
      WRITE (6,480) GAMAT
      WRITE (6,490) CLAT
      WRITE (6,530)
      WRITE (6,430) VRC1
      WRITE (6,440) VTC
      WRITE (6,540) VB1
      WRITE (6,520) VS
      WRITE (6,470) SWLEV
      WRITE (6,490) CLAV
      GO TO 110
  100 READ (5,120) STAR
C
CCCCCCCCCCCCCCCCCCCCCCCCCCCCCCCCCCCCCCCCCCCCCCCCCCCCCCCCCCCCCCCCC
C                                                               C
C  COMPUTATION OF RELEVENT LONGITUDINAL STABILITY COEFFICIENTS  C
C                                                               C
CCCCCCCCCCCCCCCCCCCCCCCCCCCCCCCCCCCCCCCCCCCCCCCCCCCCCCCCCCCCCCCCC
C
      READ (5,150) H,CLTRM
      READ (5,130) ST
      READ (5,160) TL,TH,CLAT,CMOWB
      READ (5,160) WA,WB,HNWB,SWLEW
      READ (5,160) CR1,CT,GAMAW,ALFAZL
      READ (5,160) CLAW,CLAWS,CLAM,CLAWB
      RADIAN = 57.29577D0
      SWLE = SWLEW/RADIAN
      GAMA = GAMAW/RADIAN
      AR = WB**2/WA
      TAP = CT/CR1
      TSWQC = DTAN(SWLE)-(4.D0/AR)*(.25D0*((1.D0-TAP)/(1.D0+TAP)))
      SWQC = DATAN(TSWQC)
      AK = 1.D0/AR-1.D0/(1.D0+AR**1.7)
      AL = (10.D0-3.D0*TAP)/7.D0
      POWER = 1.D0/3.D0
      AH = (1.D0-TH/WB)/(2.D0*TL/WB)**POWER
      CSWQC = DCOS(SWQC)
      DEDA = 4.44D0*(AK*AL*AH*DSQRT(CSWQC))**1.19
```

```
      OMDEDA = 1.DO-DEDA
      CBARG = ((2.DO*CR1)/3.DO)*(1.DO+TAP+TAP**2)/(1.DO+TAP)
      VH = (TL*ST)/(WA*CBARG)
      BRCKT1 = CLAT*OMDEDA/CLAWB
      BRCKT2 = VH*BRCKT1
      BRCKT3 = H*ST*BRCKT1/WA
      UP1 = HNWB+BRCKT2+BRCKT3
      DWN1 = 1.DO+BRCKT3/H
      HN = UP1/DWN1
      SFSM = HN-H
      EPSLNO = -DEDA*ALFAZL/RADIAN
      EPSLN1 = EPSLNO*RADIAN
      CMA = -CLAM*SFSM
      CMQ = -2.DO*CLAT*.9DO*VH*TL/CBARG
      CMAD = CMQ*DEDA
      CMAT = -VH*CLAT
      AR = WB**2/WA
      TSUBI = -ALFAZL/RADIAN
      PAREN1 = CLAT*TL*ST*(EPSLNO+TSUBI)/(WA*CBARG)
      PAREN2 = CLAWB*CLAT*ST*(EPSLNO+TSUBI)/(CLAM*WA)
      PAREN3 = H-HNWB
      PAREN4 = (TL*ST*CLAT*(1.DO-DEDA))/(CLAWB*WA*CBARG)
      PAREN5 = PAREN3-PAREN4
      CMOA = CMOWB+PAREN1+PAREN2*PAREN5
      CONST = TL/CBARG
      CLTRIM = CLTRM*CONST
      ALFAM = (CLTRIM-CMOA)/(CLAM*CONST+CMA)
      ALFAT = (CLTRM-CLAM*ALFAM)/(CLAT*ST/WA)
      ALFAW1 = ALFAM*RADIAN
      ALFAT1 = ALFAT*RADIAN
      ALFAWB = ALFAM+(CLAT*ST*(EPSLNO+TSUBI))/(CLAM*WA)
      CLWB = CLAWB*ALFAWB
      GO TO 90
  110 WRITE (6,550)
      WRITE (6,560)
      WRITE (6,570)
      WRITE (6,580)
      WRITE (6,590)
      WRITE (6,600)
      WRITE (6,610)
      WRITE (6,620) CMQ,CMA
      WRITE (6,630) CMAD,CMAT
C
CCCCCCCCCCCCCCCCCCCCCCCCCCCCCCCCCCCCCCCCCCCCCCCCCCCCCCCCCCCCCCCC
C                                                              C
C  COMPUTATION OF THE ELEMENTS OF THE STATE VARIABLE MATRICES  C
C                                                              C
CCCCCCCCCCCCCCCCCCCCCCCCCCCCCCCCCCCCCCCCCCCCCCCCCCCCCCCCCCCCCCCC
```

```
C
      AIX = (8.0D0*A)/(2.378D-3*WA*32.2D0*WB**3)*(12**3)
      BIY = (8.0D0*B)/(2.378D-3*WA*32.2D0*CBARG**3)*(12**3)
      CIZ = (8.0D0*C)/(2.378D-3*WA*32.2D0*WB**3)*(12**3)
      EIXZ = (8.0D0*E)/(2.378D-3*WA*32.2D0*WB**3)*(12**3)
      A11 = (CMQ+CMAD)/BIY
      A12 = CMA/BIY
      A21 = 1.0D0
      A22 = 0.0D0
      BM1 = CMAT/BIY
      BM2 = 0.0D0
      WRITE (6,640)
      WRITE (6,650) A11,A12
      WRITE (6,660) A21,A22
      WRITE (6,670)
      WRITE (6,680) BM1
      WRITE (6,680) BM2
C
CCCCCCCCCCCCCCCCCCCCCCCCCCCCCCCCCCCCCCCCCCCCCCCCCCCCCCCCCCCC
C                                                          C
C   COMPUTATION OF RELEVENT LATERAL STABILITY DERIVITIVES  C
C                                                          C
CCCCCCCCCCCCCCCCCCCCCCCCCCCCCCCCCCCCCCCCCCCCCCCCCCCCCCCCCCCC
C
      WRITE (6,550)
      WRITE (6,690)
      WRITE (6,700)
      WRITE (6,710)
      WRITE (6,720)
      WRITE (6,730)
      WRITE (6,740)
      WRITE (6,750)
      WRITE (6,760)
      WRITE (6,770)
C
C   COMPUTATUION OF CL(BETA) AND CN(BETA)
C
      READ (5,180) CLBCLS,SKM,FK,CLBCLA,CLBG,GKM
      READ (5,150) H,ZW
      RADIAN = 57.29577D0
      CLBWB1 = CLBCLS*SKM*FK+CLBCLA
      CLBWB2 = CLWB*CLBWB1
      DELCLB = -5.0D-4*AR*(DISTW/WB)**2
      CLBWB3 = CLBG*GKM+DELCLB
      CLBWB4 = GAMAW*CLBWB3
      DCLBZW = (1.2D0*DSQRT(AR)*ZW*2.D0*DISTW)/(RADIAN*WB**2)
      CLBWB = (CLBWB2+CLBWB4+DCLBZW)*RADIAN
      READ (5,180) HCBCLS,HSKM,HFK,HCBCLA,HCLBG,HGKM
```

```
      READ (5,130) ZWH
      CLTAIL = CLAT*ALFAWB*(1.DO-DEDA)-CLAT*(EPSLNO+TSUBI)
      CLBH1 = HCBCLS*HSKM*HFK+HCBCLA
      CLBH2 = CLTAIL*CLBH1
      ART = TB**2/ST
      DHCLBZ = (1.2DO*DSQRT(ART)*ZWH*2.DO*DIST)/(RADIAN*TB**2)
      DHCLBG = -5.D-4*ART*(DIST/TB)**2
      CLBH3 = HCLBG*HGKM+DHCLBG
      CLBH4 = GAMAT*CLBH3*RADIAN
      VH1 = (ST*TB)/(WA*WB)
      CLBH5 = RADIAN*(CLBH2+CLBH4+DHCLBZ)
      CLBH = VH1*CLBH5
      READ (5,170) CONSTV,CLAV,VS
      READ (5,150) ZV,VL
      CSWQC = DCOS(SWQC)
      DSDB = .724DO+3.06DO*(VS/(WA*(1.DO+CSWQC)))+.4DO*ZWH/DISTW+9.D-3*A
     1R
      CYBV = -CONSTV*CLAV*DSDB*VS/WA
      CLBV = CYBV*(ZV*DCOS(ALFAWB)-VL*DSIN(ALFAWB))/WB
      CLB = CLBWB+CLBH+CLBV
      VLC = VL*DCOS(ALFAWB)+ZV*DSIN(ALFAWB)
      ZVC = ZV*DCOS(ALFAWB)-VL*DSIN(ALFAWB)
      READ (5,160) XKN,XKRL,SBS,FL
      CNBB = -RADIAN*XKN*XKRL*SBS*FL/(WA*WB)
      CNBV = -CYBV*VLC/WB
      CNB = CNBB+CNBV
      WRITE (6,780) CLB,CNB
C
C   COMPUTATION OF CL(P) AND CN(P)
C
      READ (5,160) XBCLPK,CLAWS,HBCLPK,CLATS
      CCNW = CLAWS/(2.DO*3.14159DO)
      CCNT = CLATS/(2.DO*3.14159DO)
      CLPW = XBCLPK*CONW
      CLPH = .5DO*(HBCLPK*CONT)*(ST/WA)*(TB/WB)**2
      CLPV = 2.DO*(ZV/WB)**2*CYBV
      CLP = CLPW+CLPH+CLPV
      READ (5,130) XBAR1
      TSWQC = DTAN(SWQC)
      B7 = 1.DO
      TANOAT = DTAN(ALFAWB)
      AB7 = A*B7
      CNPW1 = -CLPW*TANOAT
      CNPW2 = -CLP*TANOAT
      CNPW31 = (AR+4.DO*CSWQC)/(AB7+4.DO*CSWQC)
      CNPW3T = AB7+.5DO*(AB7+CSWQC)*(TSWQC)**2
      CNPW3B = AR+.5DO*(AR+CSWQC)*(TSWQC)**2
      CNPW3 = (CNPW3T/CNPW3B)*CNPW31
```

```
      CNPW41 = 6.DO*(AR+CSWQC)
      CNPW42 = (XBAR1*TSWQC)/(CBARG*AR)+(TSWQC)**2/12.DO
      CNPW4T = -1.DO*(AR+CNPW41*CNPW42)
      CNPW4B = 6.DO*(AR+4.DO*CSWQC)
      CNPW4 = CNPW4T/CNPW4B
      CNPW5 = CNPW3*CNPW4
      CNPW6 = CNPW5*CLWB
      CNPW = CNPW1-(CNPW2-CNPW6)
      CNPV = -2.DO*VLC*(ZVC-ZV)*CYBV/WB**2
      CNP = CNPW+CNPV
      WRITE (6,790) CLP,CNP
C
C   COMPUTATION OF CL(R) AND CN(R)
C
      READ (5,130) XCLRCL
      CTOP1 = AR*(1.DO-B7**2)/(2.DO*B7*(AB7+2.DO*CSWQC))
      CTOP2 = ((AB7+2.DO*CSWQC)*TSWQC**2)/(8.DO*(AB7+4.DO*CSWQC))
      CTOP = 1.DO+CTOP1+CTOP2
      CBOT = 1.DO+(AR+2.DO*CSWQC*TSWQC**2)/(8.DO*(AR+4.DO*CSWQC))
      CLRW1 = (CTOP/CBOT)*XCLRCL*CLWB
      DCLRG = (3.14159DO*AR*DSIN(SWQC))/(12.DO*(AR+4.DO*CSWQC))
      CLRW = CLRW1+GAMA*DCLRG
      CLRV = -2.DO*VLC*ZVC*CYBV/WB**2
      CLR = CLRW+CLRV
      READ (5,170) XCNRCL,XCNRCD,CDO
      CNRW = XCNRCL*CLWB**2+XCNRCD*CDO
      CNRV = 2.DO*(VLC**2)*CYBV/WB**2
      CNR = CNRW+CNRV
      WRITE (6,800) CLR,CNR
C
C   COMPUTATION OF CL(DELTA-AILERON) AND CN(DELTA-AILERON)
C
      READ (5,160) BCPLDK,CLDTD,CLDT,CK
      CONSTK = CLAWS/(2.ODO*3.14159DO)
      CPLD = CONSTK*BCPLDK
      CLD1 = CLDTD*CLDT
      ALFAD = CLD1/CLAWS
      CLDEL = ALFAD*CPLD
      CLDA = 2.DO*CLDEL
      CNDA = CK*CLWB*CLDA
      WRITE (6,810) CLDA,CNDA
C
C   COMPUTATION OF CL(DELTA-FIN) AND CN(DELTA-FIN)
C
      CLDF = (CLAV*VS*ZV)/(WA*WB)
      CNDF = -(CLAV*VS*VL)/(WA*WB)
      WRITE (6,820) CLDF,CNDF
C
```

```
CCCCCCCCCCCCCCCCCCCCCCCCCCCCCCCCCCCCCCCCCCCCCCCCCCCCCCCCCCCCCCCCCCCCCCCC
C                                                                      C
C  COMPUTATION OF ELEMENTS FOR STATE VARIABLE MATRICES (LATERAL)       C
C                                                                      C
CCCCCCCCCCCCCCCCCCCCCCCCCCCCCCCCCCCCCCCCCCCCCCCCCCCCCCCCCCCCCCCCCCCCCCCC
C
      DNCMTR = AIX*CIZ-EIXZ**2
      C11 = (CIZ*CLP+EIXZ*CNP)/DNOMTR
      C12 = (CIZ*CLR+EIXZ*CNR)/DNOMTR
      C13 = (CIZ*CLB+EIXZ*CNB)/DNOMTR
      C14 = 0.0D0
      C21 = (AIX*CNP+EIXZ*CLP)/DNOMTR
      C22 = (AIX*CNR+EIXZ*CLR)/DNOMTR
      C23 = (AIX*CNB+EIXZ*CLB)/DNOMTR
      C24 = 0.0D0
      C31 = 0.0D0
      C32 = -1.0D0
      C33 = 0.0D0
      C34 = 0.0D0
      C41 = 1.0D0
      C42 = 0.0D0
      C43 = 0.0D0
      C44 = 0.0D0
      D11 = (CIZ*CLDA+EIXZ*CNDA)/DNOMTR
      D12 = (CIZ*CLDF+EIXZ*CNDF)/DNOMTR
      D21 = (AIX*CNDA+EIXZ*CLDA)/DNOMTR
      D22 = (AIX*CNDF+EIXZ*CLDF)/DNOMTR
      D31 = 0.0D0
      D32 = 0.0D0
      D41 = 0.0D0
      D42 = 0.0D0
      WRITE (6,640)
      WRITE (6,830) C11,C12,C13,C14
      WRITE (6,830) C21,C22,C23,C24
      WRITE (6,830) C31,C32,C33,C34
      WRITE (6,830) C41,C42,C43,C44
      WRITE (6,840)
      WRITE (6,850) D11,D12
      WRITE (6,850) D21,D22
      WRITE (6,850) D31,D32
      WRITE (6,850) D41,D42
      WRITE (6,550)
C
C
C
  120 FORMAT (5A4)
  130 FORMAT (F10.7)
  140 FORMAT (I2)
```

```
150 FORMAT (2F10.7)
160 FORMAT (4F10.7)
170 FORMAT (3F10.7)
180 FORMAT (6F10.4)
190 FORMAT (5F10.4)
200 FORMAT ('1 ',//////,43X,11('*****'))
210 FORMAT (43X,11('*****'))
220 FORMAT (43X,11('*****'),////)
230 FORMAT (43X,'**',51X,'**')
240 FORMAT (43X,'**',15X,'MODEL CHARACTERISTICS',15X,'**')
250 FORMAT (59X,'TOTAL MODEL PARAMETERS:')
260 FORMAT (59X,'-',11('--'),////)
270 FORMAT (48X,'TRIM LIFT COEFFICIENT (CL) =    ',1PD14.7,//)
280 FORMAT (48X,'MODEL ANGLE OF ATTACK (DEG.) = ',1PD14.7,//)
290 FORMAT (48X,'TAIL ANGLE OF ATTACK (DEG) =    ',1PD14.7,//)
300 FORMAT (48X,'TOTAL LENGTH (IN) = ',11X,1PD14.7,//)
310 FORMAT (48X,'TOTAL WEIGHT (LBS) = ',10X,1PD14.7,//)
320 FORMAT (48X,'STICK FIXED STATIC MARGIN = ',3X,1PD14.7,//)
330 FORMAT (48X,'LIFT CURVE SLOPE (PER RAD.) =   ',1PD14.7,/////)
340 FORMAT (57X,'MOMENTS OF INERTIA (IN2-LBS)',//)
350 FORMAT (47X,'I(X) = ',1PD14.7,5X,'I(Y) =  ',1PD14.7,//)
360 FORMAT (47X,'I(Z) = ',1PD14.7,5X,'I(XZ) = ',1PD14.7,/////)
370 FORMAT (44X,'MODEL C.G. WITH RESPECT TO REFERENCE AXIS ORIGIN (IN)
   1',//)
380 FORMAT (47X,'XBAR = ',1PD14.7,5X,'YBAR =  ',1PD14.7,//)
390 FORMAT (47X,'ZBAR = ',1PD14.7,//)
400 FORMAT ('1 ',///////,54X,'WING AND TAIL SURFACE PARAMETERS:')
410 FORMAT (54X,'-',11('---'),////)
420 FORMAT (59X,'-WING CHARACTERISTICS-',//)
430 FORMAT (48X,'ROOT CHORD (IN) = ',12X,1PD14.7,//)
440 FORMAT (48X,'TIP CHORD (IN) = ',13X,1PD14.7,//)
450 FORMAT (48X,'WING SPAN (IN) = ',13X,1PD14.7,//)
460 FORMAT (48X,'WING AREA (IN2) = ',12X,1PD14.7,//)
470 FORMAT (48X,'L.E. SWEEP (DEG) = ',11X,1PD14.7,//)
480 FORMAT (48X,'DIHEDRAL ANGLE (DEG) = ',7X,1PD14.7,//)
490 FORMAT (48X,'LIFT CURVE SLOPE (PER RAD) =  ',1PD14.7,/////)
500 FORMAT (54X,'-HORIZONTAL TAIL CHARACTERISTICS-',//)
510 FORMAT (48X,'TAIL SPAN (IN) = ',13X,1PD14.7,//)
520 FORMAT (48X,'TAIL AREA (IN2) = ',12X,1PD14.7,//)
530 FORMAT ('1 ',/////////,55X,'-VERTICAL TAIL CHARACTERISTICS-',//)
540 FORMAT (48X,'TAIL HEIGHT (IN) = ',11X,1PD14.7,//)
550 FORMAT ('1 ',///////)
560 FORMAT (53X,'LONGITUDINAL STABILITY DERIVATIVES:')
570 FORMAT (53X,7('-----'),//)
580 FORMAT (48X,'CM- = VARIATION OF PITCHING MOMENT COEFFICIENT',/)
590 FORMAT (54X,'WITH -',/)
600 FORMAT (48X,'A = ANGLE OF ATTACK (ALFA)',4X,'Q = PITCH RATE',/)
610 FORMAT (48X,'A(DOT) = VARIATION OF ALFA WITH RESPECT TO TIME',////
```

```
     1//)
 620 FORMAT (43X,'CMQ = ',5X,1PD14.7,4X,'CMA = ',6X,1PD14.7,//)
 630 FORMAT (43X,'CMA(DOT) = ',1PD14.7,4X,'CMA(TAIL) = ',1PD14.7,/////)
 640 FORMAT (43X,'ELEMENTS OF STATE VARIABLE MATRIX A ARE:',//)
 650 FORMAT (54X,1PD14.7,5X,1PD14.7,/)
 660 FORMAT (54X,1PD14.7,5X,1PD14.7,/////)
 670 FORMAT (43X,'ELEMENTS OF THE B VECTOR ARE:',//)
 680 FORMAT (64X,1PD14.7,/)
 690 FORMAT (56X,'LATERAL STABILITY DERIVATIVES:')
 700 FORMAT (56X,10('---'),//)
 710 FORMAT (48X,'CL- = VARIATION OF ROLLING MOMENT COEFFICIENT',/)
 720 FORMAT (54X,'WITH -',/)
 730 FORMAT (48X,'CN- = VARIATION OF YAWING MOMENT COEFFICIENT',/)
 740 FORMAT (54X,'WITH -',/)
 750 FORMAT (48X,'B = SIDESLIP ANGLE (BETA)',/)
 760 FORMAT (48X,'P = ROLL RATE',17X,'R = YAW RATE',/)
 770 FORMAT (48X,'DA = AILERON DEFLECTION',7X,'DF = RUDDER DEFLECTION',
     1////)
 780 FORMAT (45X,'CLB =  ',1PD14.7,10X,'CNB =  ',1PD14.7,//)
 790 FORMAT (45X,'CLP =  ',1PD14.7,10X,'CNP =  ',1PD14.7,//)
 800 FORMAT (45X,'CLR =  ',1PD14.7,10X,'CNR =  ',1PD14.7,//)
 810 FORMAT (45X,'CLDA = ',1PD14.7,10X,'CNDA = ',1PD14.7,//)
 820 FORMAT (45X,'CLDF = ',1PD14.7,10X,'CNDF = ',1PD14.7,////)
 830 FORMAT (42X,4(1PD14.7,4X),/)
 840 FORMAT (////,43X,'ELEMENTS OF THE B MATRIX ARE:',//)
 850 FORMAT (54X,2(1PD14.7,5X),/)
     END
```

LIST OF REFERENCES

1. Etkin, Bernard, Dynamics of Flight - Stability and Control, John Wiley and Sons, New York, 1959.

2. Hess, R. A., "Introduction to Modern Control Theory," Naval Postgraduate School, Monterey, California, 1974 (mimeographed).

3. Roskam, J., Methods for Estimating Stability and Control Derivatives of Conventional Subsonic Airplanes, published by the author, 519 Boulder, Lawrence, Kansas, 1971.

INITIAL DISTRIBUTION LIST

		No. Copies
1.	Defense Documentation Center Cameron Station Alexandria, Virginia 22314	2
2.	Library, Code 0212 Naval Postgraduate School Monterey, California 93940	2
3.	Chairman, Department of Aeronautics, Code 57 Naval Postgraduate School Monterey, California 93940	1
4.	Professor H. L. Power, Jr., Code 57 Ph Department of Aeronautics Naval Postgraduate School Monterey, California 93940	1
5.	ENS John Christian Merrill, USN 6816 Ross Road Springwater, New York 14560	2

161018
Thesis
M537 Merrill
c.1 A remotely controlled wind tunnel model for the demonstration of aircraft stability and control characteristics.